TÜRKİYE CUMHURİYETİ
ADANA ALPARSLAN TÜRKEŞ SCIENCE AND TECHNOLOGY UNIVERSITY

GRADUATE SCHOOL
BIOENGINEERING DEPARTMENT

GSK2126458 LOADED POLYCAPROLACTONE (PCL)/POLYVINYLPYRROLIDONE (PVP) ELECTROSPUN MEMBRANES: PRODUCTION, CHARACTERIZATION AND ANTICANCER ACTIVITY

ALİCAN CÖMERTPAY

M.Sc.

ADANA 2024

TÜRKİYE CUMHURİYETİ
ADANA ALPARSLAN TÜRKEŞ SCIENCE AND TECHNOLOGY UNIVERSITY

GRADUATE SCHOOL
BIOENGINEERING DEPARTMENT

GSK2126458 LOADED POLYCAPROLACTONE (PCL)/POLYVINYLPYRROLIDONE (PVP) ELECTROSPUN MEMBRANES: PRODUCTION, CHARACTERIZATION AND ANTICANCER ACTIVITY

ALİCAN CÖMERTPAY

M.Sc.

THESIS ADVISOR
ASSOC. PROF. DR. MERVE ÇAPKIN YURTSEVER

SECOND ADVISOR
ASSOC. PROF. DR. ZEYNEP İYİGÜNDOĞDU

ADANA, 2024

DECLARATION OF CONFORMITY

In this thesis study, which was prepared following the thesis writing rules of Adana Alparslan Türkeş Science and Technology University Institute of Graduate School, I declare that I provide all the information, documents, evaluations and results in accordance with scientific ethics and moral codes without resorting to any means or assistance that would be contrary to scientific ethics and traditions. I also declare that I refer to all of the articles I used in this study with appropriate references and accept all moral and legal consequences if a situation is found contrary to my statement regarding my work.

..../..../20..

Alican CÖMERTPAY

ÖZET

GSK2126458 YÜKLÜ POLİKAPROLAKTON (PCL) / POLİVİNİLPRROLİDON (PVP) ELEKTROEĞRİLMİŞ MEMBRANLAR: ÜRETİM, KARAKTERİZASYON VE ANTİKANSER AKTİVİTE

Alican CÖMERTPAY
Yüksek Lisans, Biyomühendislik Anabilim Dalı
Danışman: Doç. Dr. Merve ÇAPKIN YURTSEVER
II. Danışman: Doç. Dr. Zeynep İYİGÜNDOĞDU
Temmuz 2024, 91 sayfa

Deri kanseri, en tehlikeli kanser türlerinden biridir. Deri hücrelerinde oluşan DNA hasarının giderilememesiyle ortaya çıkan mutasyonlar sonucunda deride kanserli doku oluşumu görülebilmektedir. Deri kanseri insan vücudunda farklı bölgelere yayılma gösterebilen bir kanser türüdür ve iki ana gruba ayrılmaktadır: melanom ve melanom olmayan. Literatürdeki veriler melanom kanser türünün, deri kanseri vakalarının %1'ini oluşturduğunu belirtmektedir. Melanom deri kanserinin görülme sıklığı düşük olmasına rağmen hastaların ölüm oranları yüksektir. Deri kanseri tedavisinde farklı metotlar bulunmaktadır. Bu metotlardan en yaygın olanı biyopsi ve rezeksiyondur. Son yıllarda deri kanseri tedavisinde nanoteknoloji kullanımına ilgi artmıştır. Nanoteknoloji ile üretilen malzemeler molekül taşıyıcıları olarak kullanılmaktadır. Nanoteknolojik yöntemler kullanılarak üretilmiş membranlar ile ilacın spesifik bölgeye direkt uygulanabilmesi, daha hızlı tedavi ve azaltılmış yan etkiler elde edilmesi amaçlanmaktadır.

Bu çalışmada, kanser ilacı olarak kullanılan GSK2126458 (Omipalisib®) ilacının elektroeğirme yöntemi ile elde edilen Polikaprolakton (PCL)/ Polivinilprolidon (PVP) fiber membranlar içerisine yüklenmesi ve melanom kanser hücre hattı üzerindeki etkilerinin incelenmesi amaçlanmıştır. Çalışma kapsamında elektroeğirme yöntemi ile GSK2126458 ilacını içeren, PCL/PVP/50 (50 µL ilaç ve 50 µL DMSO), PCL/PVP/75 (75 µL ilaç ve 25 µL DMSO) ve PCL/PVP/100 (100 µL ilaç) ve içermeyen PCL/PVP/C fiber membranlar üretilmiştir. Tüm örneklerde DMSO oranı sabit tutulmuştur. Üretilen fiber yapıların morfolojileri taramalı electron mikroskobu (SEM) ile kimyasal yapıları Fourier Transform

Infrared Spectroscopy (FTIR) analizleri ile gerçekleştirilmiştir. Fiber çapları ve çap dağılımları SEM analizi ile elde edilen görüntülerden ImageJ program ile hesaplanmıştır. Fiber membranların su tutma özellikleri su temas açısı analizi ile mekanik özellikleri çekme-germe analizi ile belirlenmiştir. Üretilen fiber membranların antibakteriyel özelliklerinin belirlenmesi için *E. coli, S. aureus, P. aeruginosa* ve *MRSA* bakteri suşları üzerinde mikrobiyolojik analizler gerçekleştirilmiştir. Fiberlerin içerisine yüklenen GSK2126458 ilacının B16-F10 hücre hattı üzerindeki IC_{50} değeri resazurin analizi ile belirlenmiştir. İlacın fiber membrana eklendikten sonra melanom hücreleri üzerinde etkili olup olmadığı canlılık analizi, hücre morfolojisinin ve yayılma davranışının SEM analizi görüntülenmesi ve immünofloresan boyama ile araştırılmıştır.

Tez çalışması sonucunda, GSK2126458 ilaç molekülü yüklenmiş ve ilaç içermeyen kontrol fiber membranlar düzgün ve boncuk içermeyen fiber yapısında elde edilmiştir. PCL/PVP/C, PCL/PVP/50, PCL/PVP/75 ve PCL/PVP/100 fiber gruplarının fiberlerinin ortlama çapları sırasıyla, 0.682±0,316, 0.588±0.240, 0.637±0.208 ve 0.611±0.196 μm olarak belirlenmiştir. PCL/PVP/C, PCL/PVP/50, PCL/PVP/75 ve PCL/PVP/100 fiber gruplarının su temas açısı analizleri sonucunda sırasıyla, 76.02±8.06, 83.63±1.75, 66.98±2.83 ve 82.92±12.82 dereceleri elde edilmiştir ve membranların hidrofilik yapıları gösterilmiştir. FTIR analizi ile PCL ve PVP polimerlerine spesifik pikler gösterilmiştir ancak ilaç molekülü için spesifik bir pik ilacın polimer yapısına gömülü olmasından dolayı elde edilememiştir. GSK2126458 ilacının B16-F10 fare melanom hücre hattı üzerinde IC_{50} değeri 49.21 μM olarak belirlenmiştir. İlaç yüklü membranlardaki hücre canlılığı ilaç içermeyen fiber membranlara göre analiz edildiğinde PCL/PVP/50, PCL/PVP/75 ve PCL/PVP/100 fiber membranlarda hücre canlılığının 24 saat için sırasıyla %72.25, %64.61 ve %57.82 ($p<0.05$) oldukları belirlenmiştir. 48 saat için ise sırasıyla, %74.76, %70.85 ($p<0.05$) ve %60.19 ($p<0.01$) oldukları belirlenmiştir. SEM görüntülerinde hücre yayılmasının kontrol grubunda diğer gruplara göre daha belirgin olduğu gösterilmiştir. Fiber membranlar üzerinde kültüre edilen hücrelerin fibröz aktin proteinin anti F-aktin antikoru ve çekirdeğinin DAPI ile boyanması ile elde edilen immünofloresan boyama görüntülerinde hücre yoğunluğunun artan ilaç molekülü miktarı ile azaldığı gösterilmiştir. Hücre çekirdeğinde belirgin değişiklikler görülmemiştir. Sonuç olarak, GSK2126458 ilacı yüklü PCL/PVP fiber membranların tez çalışması kapsamında başarı ile üretildiği ve B16-F10 fare melanom hücre hattı üzerinde etkili olduğu gösterilmiştir.

Anahtar kelimeler: Melanom, GSK2126458, nanofiber, PCL, PVP

ABSTRACT

GSK2126458 LOADED POLYCAPROLACTONE (PCL)/POLYVINYLPYRROLIDONE (PVP) ELECTROSPUN MEMBRANES: PRODUCTION, CHARACTERIZATION AND ANTICANCER ACTIVITY

Alican CÖMERTPAY

M.Sc., Department of Bioengineering

Supervisor: Assoc. Prof. Dr. Merve ÇAPKIN YURTSEVER

Co-Supervisor: Assoc. Prof. Dr. Zeynep İYİGÜNDOĞDU

July 2024, 91 pages

Skin cancer is one of the most dangerous cancers. The mutations resulting from the failure to repair DNA damage in skin cells result in the formation of cancer tissue in the skin. Skin cancer is a type of cancer that can spread to different parts of the human body and is divided into two main groups: melanoma and non-melanoma. The data in the literature indicate that the type of melanoma cancer accounts for 1% of cases of skin cancer. Although the incidence of melanoma skin cancer is low, patients have high mortality rates. There are different methods of treating skin cancer. The most common of these methods are biopsy and resection. In recent years, interest in the use of nanotechnology in the treatment of skin cancer has increased. Materials produced by nanotechnology are used as molecular carriers. Membranes produced using nanotechnological methods are intended to enable the drug to be applied directly to a specific area, to faster treatment and to reduce side effects.

In this study, it was aimed to load GSK2126458 (Omipalisib®), which is used as a cancer drug, into Polycaprolactone (PCL)/ Polyvinylprolidone (PVP) fiber membranes obtained by electrospinning method and to investigate its effects on melanoma cancer cell line. Within the scope of the study, PCL/PVP/50 (50 µL drug and 50 µL DMSO), PCL/PVP/75 (75 µL drug and 25 µL DMSO), PCL/PVP/100 (100 µL drug) and PCL/PVP/C fiber membranes containing GSK2126458 drug and PCL/PVP/C fiber membranes without drug were produced by electrospinning method. DMSO ratio was kept constant in all samples. The morphology of the produced fiber structures were analyzed by scanning electron microscopy (SEM) and their

chemical structures were analyzed by Fourier Transform Infrared Spectroscopy (FTIR). Fiber diameters and diameter distributions were calculated from the images obtained by SEM analysis using ImageJ software. Water retention properties of the fiber membranes were determined by water contact angle analysis and mechanical properties were determined by tensile analysis. Antibacterial properties of the fiber membranes were determined using *E. coli, S. aureus, P. aeruginosa* and *MRSA* bacterial strains. The IC50 value of the GSK2126458 on B16-F10 cell line was determined by resazurin assay. The effect of the drug on melanoma cells after being added to the fiber membrane was determined by viability analysis, SEM analysis of cell morphology and spreading behavior and immunofluorescent staining.

As a result of the thesis study, GSK2126458 drug molecule loaded and drug-free control fiber membranes were obtained in a smooth and bead-free fiber structure. The average diameters of the fibers of PCL/PVP/C, PCL/PVP/50, PCL/PVP/75 and PCL/PVP/100 membranes were calculated as 0.682±0,316, 0.588±0.240, 0.637±0.208 ve 0.611±0.196 μm, respectively. Hydrophilic structures of the membranes were shown by water contact angles of 76.02±8.06, 83.63±1.75, 66.98±2.83 ve 82.92±12.82 degrees for PCL/PVP/C, PCL/PVP/50, PCL/PVP/75 and PCL/PVP/100 fiber membranes, respectively. FTIR analysis showed specific peaks for PCL and PVP polymers, but a specific peak for the drug molecule could not be obtained because the drug was embedded in the polymer structure. The IC50 value of GSK2126458 on B16-F10 cell line was determined as 49.21 μM. When cell viability in drug-loaded membranes was analyzed compared to drug-free fiber membranes, it was determined that cell viability in PCL/PVP/50, PCL/PVP/75 and PCL/PVP/100 fiber membranes were 72.25%, 64.61% and 57.82% ($p<0.05$) for 24 hours, respectively. The viabilities were changed to 74.76%, 70.85% ($p<0.05$) and 60.19% ($p<0.01$) for 48 h, respectively. SEM images showed that cell spreading was more prominent in the control group than in the other groups. Immunofluorescence staining images obtained by staining fibrous actin protein of cells cultured on fiber membranes with anti F-actin antibody and nuclei with DAPI showed that cell density decreased with increasing amount of drug molecule. No significant changes were observed in the cell nucleus. In conclusion, it was shown that GSK2126458 drug loaded PCL/PVP fiber membranes were successfully produced within the scope of the thesis study and were effective on B16-F10 mouse melanoma cell line.

Keywords: Melanoma, GSK2126458, nanofiber, PCL, PVP

ACKNOWLEDGEMENTS

I would like to thank and express my gratitude and my respect to my academic advisors Assoc. Prof. Dr. Merve ÇAPKIN YURTSEVER and Assoc. Prof. Dr. Zeynep İYİGÜNDOĞDU for supporting me with their knowledge, experience and believed in me throughout my graduate education.

I would also like to thank and express my gratitude and my respect to Asst. Prof. Özgür Cem ERKİN, who always gave me his knowledge, support and believed in me.

I would like to express my endless gratitude, appreciation, love and my deepest thanks to my mother Esen CÖMERTPAY, my father İsmail CÖMERTPAY, my sister Hande CÖMERTPAY YAĞ and my family members who have always supported me financially and morally throughout my academic life.

I would like to thank my friends, Sertay TAŞKAYA, Arda ZEYTUN, Barış TÜZEL, Ömer Faruk ERCEYLAN and Murat İDİKUT, who have always been there for me in my good and bad days and whose support I have always felt throughout my academic life.

Thanks to TÜBİTAK for awarding me a National Scholarship in Priority Fields in Science-2210/C Fellowship, providing me with the financial means to complete this thesis.

This thesis was financially supported by ATU BAP Coordination Unit with project number of 22303013.

TABLE OF CONTENTS

LIST OF FIGURES

LIST OF TABLES

LIST OF ABBREVIATIONS

5-FU	: 5-fluorouracil
ACA	: Average contact angle
AD	: Average diameter
AKT	: A serine/threonine protein kinase
Avg	: Average
BSA	: Bovine serum albumin
DAPI	: 4', 6-diamidino-2-feniliindol dihydrochloride
DCM	: Dichloromethane
DMEM-HG	: Dulbecco's modified Eagle's medium – high glucose
DMF	: Dimethylformamide
DMSO	: Dimethyl sulfoxide
DNA	: Deoxyribonucleic acid
FBS	: Fetal bovine serum
FDA	: US Food and Drug Administration
FTIR	: Fourier transform infrared
HMDS	: Hexamethyldisilazane
MRSA	: Methicillin-resistant Staphylococcus aureus
mTOR	: Mammalian target of rapamycin
MTT	: 3-(4,5-Dimethylthiazol-2-yl)-2,5-Diphenyltetrazolium Bromide
MW	: Molecular weight
MWCNT	: Multi-walled carbon nanotube
NA	: Nutrient agar
NCM	: Neurocutaneous melanocytosis
NPC	: Nasopharyngeal carcinoma
OCT	: Optical coherence tomography
P/S	: Penicillin/Streptomycin
PBS	: Phosphate buffer solution
PCL	: Polycaprolactone
PI3K	: Phosphoinositide 3-kinase
PVA	: Polyvinyl alcohol

PVP	: Polyvinylpyrrolidone
RCM	: Reflectance confocal microscopy
SD	: Standard deviation
SEM	: Scanning electron microscope
SSE	: Self skin examination
THF	: Tetrahydrofuran
UV	: Ultraviolet

LIST OF SYMBOLS

cm	**:** Centimeter
g	**:** Gram
h	**:** Hour
kV	**:** Kilovolt
M	**:** Molar
min	**:** Minute
mL	**:** Milliliter
mM	**:** Millimolar
nm	**:** Nanometer
µL	**:** Microliter
µM	**:** Micromolar
µm	**:** Micrometer

1. INTRODUCTION

It has been stated that there are 55,500 deaths per year due to cutaneous melanoma, a type of skin cancer. The incidence and mortality rates for this disease vary worldwide. The factors that cause these differences are the time of diagnosis and access to health services. If melanoma spreads, it quickly becomes a threat to human life. In recent years, thanks to the increased access to and use of innovative therapeutic agents, promising results have begun to be obtained in the treatment of solid tumors such as advanced melanoma. Within the scope of the proposed master's thesis project, the characterization of polycaprolactone (PCL) / polyvinylpyrrolidone (PVP) nanofiber structures to be obtained by electrospinning method loaded with GSK2126458 (Omipalisib®) drug molecule and its effect on the B16-F10 mouse melanoma cell line was investigated.

The B16-F10 cell line was isolated from the skin tissue of a melanoma mouse. It is a cell line that exhibits the morphology of epithelial-like cells and is used in melanoma skin cancer research. The GSK2126458 molecule is a potent and selective inhibitor of class 1 PI3K enzymes and mammalian target of rapamycin (mTOR). The GSK2126458 molecule is also reported to have antiproliferative effects on melanoma cells. PCL and PVP are biodegradable synthetic polymers that have attracted considerable attention in recent years. These two polymers have been used in various studies to be used as carriers for therapeutic molecules and to provide controlled release. While PCL provides structural strength to the material it is in, PVP provides the necessary environment for drug release.

In this thesis study, it was aimed to produce GSK2126458 drug loaded PCL/PVP nanofiber membranes and to investigate their effect on B16-F10 mouse melanoma cell line. GSK2126458/PCL/PVP and PCL/PVP membranes were produced by electrospinning method and the chemical properties of the membranes were investigated by Fourier transform infrared spectroscopy (FTIR) and the surface morphologies were investigated by scanning electron microscopy (SEM). The mechanical properties of PCL/PVP nanofibers containing GSK2126458 molecule were determined by tensile analysis and the hydrophilicity properties of the nanofibers were determined by water contact angle analysis. In addition, the antibacterial properties of the nanofibers were determined by microbiological analyses. B16-

F10 cell line were incubated on PCL/PVP nanofibers containing different amounts of GSK2126458 molecules and in culture medium containing different concentrations of GSK2126458 in a standard cell culture system. The response of cells to different concentrations of GSK2126458 drug molecules and cell viabilities on PCL/PVP nanofibers were determined by resazurin analysis and cell morphology were examined by F-actin/DAPI immunofluorescence staining methods. The morphologies of B16-F10 cells cultured on PCL/PVP nanofiber groups containing different GSK2126458 molecules were also examined by SEM analysis.

2. THEORETICAL FOUNDATIONS AND LITERATURE REVIEW

2.1. The Skin

Largest organ is the skin, in the human body. It has been reported that it constitutes 8% of the total human body weight in adult persons and has a surface area of 1.8 m^2. The skin organ has multiple functions. The skin acts as a barrier, preventing the entry of pathogens into the body. It is a sensory organ, also functions as water withholding and body temperature regulator. The skin has been reported as a model organ of great interest for testing innovations in the field of regenerative medicine based on its ability to regenerate skin tissue for wounds. The complete renewal process takes approximately 1 day. But this time depends on the parameters. With the possibility of drug absorption from the skin surface, locally and systemically drug delivery studies in skin diseases attract great attention. The skin surface has an acidic structure with a pH value between 4.2-5.6. This pH level can be affected by sweat, humidity, gender and anatomical regions. The skin structure consists of two main layers; dermis and epidermis layers. Epidermis is the structure containing keratinocytes, corneocytes and stratum corneum cells. There is a basement membrane enclosed by a lipid matrix between the epidermis and dermis structures. The dermis consists of blood vessels, nerves, lymphatic system and different cell types [1].

The epidermis layer is constantly renewed. It also forms structures such as sweat glands, hair follicles and nails. Epidermal cells are largely composed of keratinocytes, and this rate has been reported to be 80%. The differentiation process of the cells is carried out by cell migration from the basal layer to the skin surface. At the end of this differentiation process, keratinization occurs, which leads to organelle loss in the cells. The epidermis layer is divided into four separate layers due to keratinocyte differentiation, respectively; basal (*stratum germinatum*), squamous (*stratum spinosum*), granular (*stratum granulosum*) and horny layer (*stratum corneum*). The dermis layer is a layer that can be considered acellular compared to the epidermis layer. It is a tissue layer that consists primarily of type 1 and type 2 collagen protein and elastic fibers called elastin. The dermis layer contains mostly fibroblast cells, but in addition to fibroblast cells, there are also nerve and vascular networks, lymphocytes,

Schwann, fat and stem cells. The dermis layer is the main constituent of the skin. It provides elasticity to the skin, thermal regulation to the body and protects the body against mechanical damage that may come from outside. The third layer of the skin organ, the hypodermis layer, is the layer that connects the skin to the organs underneath. This layer has larger nerves and blood vessels than the dermis layer. The hypodermis layer is primarily composed of fat and fibroblast cells and macrophages. The thickness of this layer varies according to gender and location in the body. It is seen between 1.9-7.1 mm and is stated as the thickest layer of the skin [2].

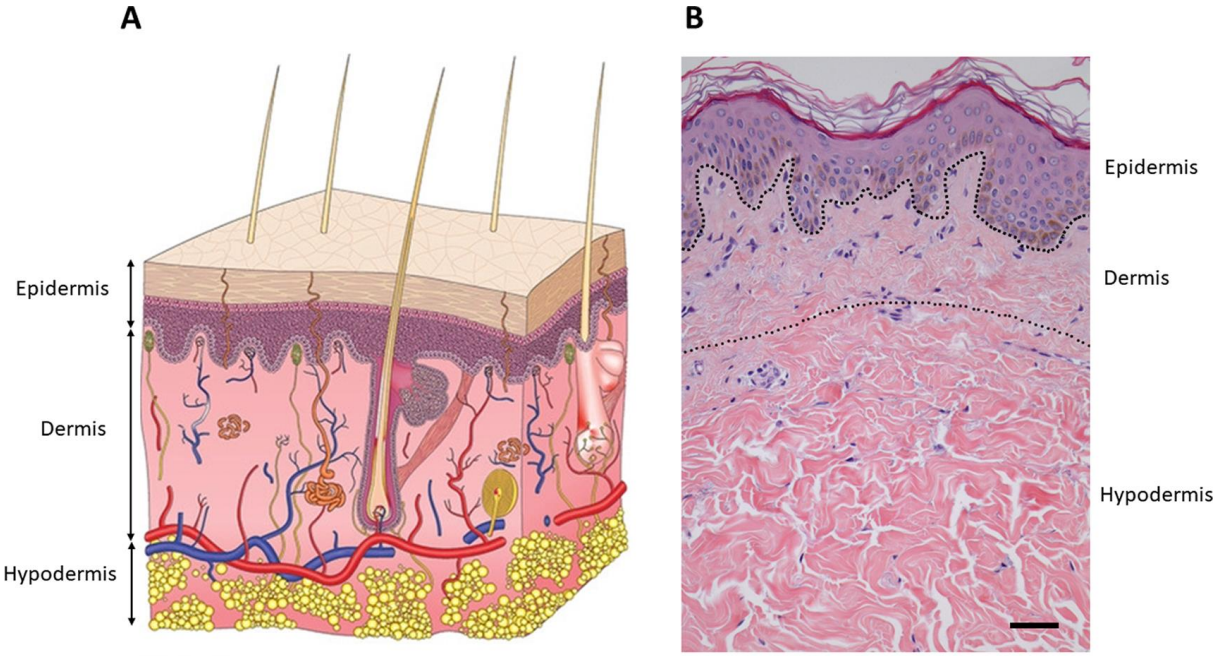

Figure 2.1. (A) Schematic view of the skin layers. (B) Histological section view of the skin layers [2].

2.2. Skin Cancer

Skin cancer is given as an example as one of the most dangerous types of cancer. It occurs as a result of unrepaired DNA in skin cells. As a result of this irreparable DNA damage, it causes deterioration, damage on the skin and mutation in the skin cells. Skin cancer have a tendency to spread to other sections of the body. Skin cancer is easily detected in the early stages and therefore easily treated in early diagnosis. With the rising rate of skin cancer cases and high mortality rate, it needs to be diagnosed early. Moreover, it is seen as a disease whose treatment process is expensive. Due to these serious problems, researchers mostly focus on

early diagnosis research. Since the skin as the largest organ, it is reported as the most frequent type of cancer. Skin cancer is divided into two major types: melanoma and non-melanoma skin cancer. In accordance with the American Cancer Society, although melanoma cases are only 1% of skin cancer cases, it is considered the most dangerous skin cancer. The reason for this is that melanoma is considered a rare but fatal type of cancer because it has high mortality rates. Doctors generally prefer the biopsy method to diagnose skin cancer. This method involves taking a tissue sample from a skin lesion thought to be cancerous and examining this tissue using correct methods. This method is seen as a painful and time-consuming method. As a result of recent studies, computer-based technologies are used to eliminate this painful situation and improve the time-consuming method [3].

There are two main layers that make up the skin organ in the human body: epidermis and dermis. The epidermis layer consists of melanocytes, Merkel, keratinocytes and Langherhans cells and constitutes the outermost and protective stratum of the skin. Any defect in this layer of the skin causes many health problems, especially skin cancer. Non-melanoma type of skin cancer is a global health problem. It has been stated that 2-3 million cases of this skin cancer develop globally every year. Its incidence is high and diverse in the Caucasian demographics globally. The data obtained indicate that the annual growth rate in America, Canada, Europe and Australia varies between 3% and 8% and shows an upward trend [4].

2.3. Melanoma

The type of cancer that develops from cells called melanocytes is called melanoma. Melanomas begin when healthy melanocytes lose control due to genetic or external factors and begin to form a cancerous tumor. It has been stated that melanoma is usually seen in areas of the body that are frequently exposed to sunlight. These areas are specified as face, neck and hands. As with every type of cancer, early diagnosis is very important in melanoma cancer type. Since melanoma is a type of cancer that can spread, it can spread to other parts of the skin organ. Therefore, skin cancer can be treated as a result of early diagnosis. Otherwise, cancer that has migrate to other sections of the body may result in a painful death of the patient [3].

It is stated that the most lethal type of skin cancer is cutaneous malignant melanoma. Epidermal melanocytes are believed to be the source of this type of cutaneous melanoma cancer. It is a type of cancer that can become resistant to treatment and tends to metastasize. There has been a remarkable increase in the number of cases recently. It has been stated that it is generally seen on the upper body in men and on the legs, ankles and feet in women. Apart from these areas, it has also been reported to be seen in the head area, neck area and other parts of the body. If melanoma is diagnosed in its early stages, it can be treated by removing it from the area with a surgical operation without the need for an additional procedure. Cutaneous melanoma has a high ability to metastasize. Recently, the use of targeted therapies and immunotherapy for this disease has become common [4].

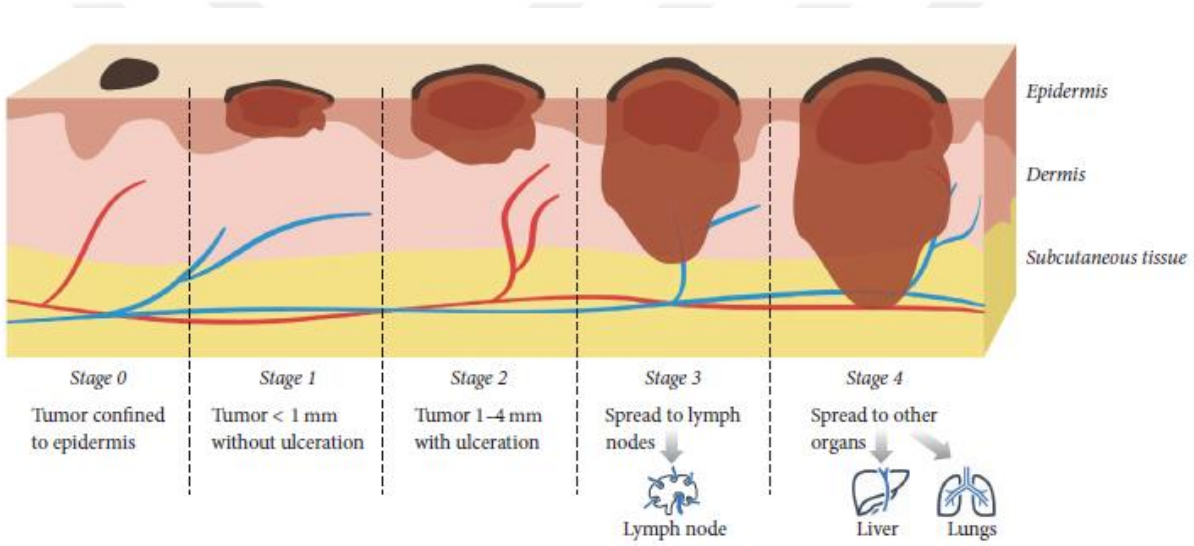

Figure 2.2. Schematic view of the five stages of malignant melanoma [5].

Melanocytes are mostly found in the skin in the human body, but they are also found in different regions such as the eyes, ears, mouth, genital and sinonasal mucosa, leptomeninges surrounding the central nervous system, and the gastrointestinal tract. Cutaneous melanoma has been reported to account for the majority of melanoma diagnoses, mostly in white people. Although exposure to UV radiation is the main cause of cutaneous melanoma cases, it has been reported that there are also rare subtypes that occur unrelated to UV radiation [6].

The most common type of cancer worldwide is skin cancer. Its incidence continues to increase day by day. It is divided into two groups as melanocytes and non-melanoma skin

cancers. These two groups constitute 95% of skin cancers. The prevalence of skin cancer is proof that this disease is an important health problem. The combination of environmental and genetic factors plays a role in the emergence of skin cancer. The most common cause of skin cancer is prolonged exposure to ultraviolet (UV) light [7].

The National Cancer Organization has stated that there is an average 1.5-fold increase in new melanoma cases each year. The organization also stated that despite this increase in the number of cases, melanoma-related death rates decreased by an average of 2.9 per year. It has been stated that the primary reason for this decrease is the early diagnosis of cancer [8].

Melanoma can be seen in the human body, especially in the skin, eyes, inner ear and leptomeninges. It is seen as a result of mutations in melanocytes, known as pigment-producing cells. Melanoma accounts for approximately 1 percent of malignant skin tumors. Additionally, the most aggressive and lethal form of skin cancer is cutaneous malignant melanoma. This disease affects both genders, especially the population living in the Caucasus region. Additionally, this disease has a poor prognosis when it becomes metastatic. In recent years, the US Food and Drug Administration (FDA) has approved different treatments. Surgical resection, radiotherapy, chemotherapy, immunotherapy or targeted therapy can be given as examples of these treatments, depending on the characteristics of the tumor. Approximately 70 percent of cutaneous melanoma cases involve mutations in genes in signaling pathways. These oncogenic mutations may be incorporated with melanoma cell proliferation. The targeted therapy approach uses inhibitors that affect proteins that have changed as a result of mutation. Phosphoinositide 3-kinase (PI3K), a serine/threonine protein kinase (AKT) and mammalian target of rapamycin (mTOR) pathway inhibitors can be given as examples of these inhibitors. mTOR plays an important role in tumor growth and progression to advanced stages. mTOR forms two different protein complexes, mTOR complex 1 and mTOR complex 2, and these protein complexes are activated by the PI3K/AKT pathway. Individually, PI3K inhibitor and mTOR inhibitor combinations have the effect of blocking the growth of melanoma cells. As a result of the studies, it is stated that PI3K-AKT pathway inhibitors show an increase in the rate of apoptosis compared to BRAF and MEK inhibitors [9].

2.3.1. Genetic Factors

Skin color of the patient is important in skin cancer. People with red hair and freckled skin carry two copies of the R allelic variant of the MC1R gene. These people have a higher risk of developing skin cancer. Xeroderma pigmentosa is an occasional autosomal recessive condition. It is a DNA repair mechanism disorder in which the ability to repair the damage caused by UV light is damaged. People with this disorder are more prone to freckling, an increase in skin malignancies in early childhood, and sunburn, it is thought that 90% of emerging melanomas occur sporadically, but inherited mutations have been described recently. The most common cause of hereditary melanomas is a mutation in the CDKN2A gene. In addition, mutations in the MDM2 gene cause melanoma to be seen at an early age in women [7].

2.3.2. Environmental Factors

The main risk cause of environmental factors has been stated as exposure to UV rays. Additional risk factors for skin cancer include more than 50 naevi, dysplastic naevi, and multiple atypical naevi, immunosuppression (especially in transplant patients), arsenic exposure, and viral infections (human papillomavirus) [7].

2.4. Types of Melanoma

There are many types of melanoma skin cancer, such as nodular, superficial spreading melanoma and lentigo maligna. However, the majority of skin cancers are non-melanoma types, such as basal cell carcinoma, squamous cell carcinoma and sebaceous gland carcinoma. Non-melanoma cancer type has a lower tendency to spread to other parts of the body and is stated to be easier to treat compared to melanoma cancer type [3].

Melanoma can be classified anatomically based on the location of the primary tumor in the body. Cutaneous melanoma generally arises from melanocytes located in the epidermal layer. It has also been reported to originate less frequently from the dermal layer, other than the epidermal layer. Acral melanoma is seen in the hands and soles. Ocular melanoma is a general term that can develop from melanocytes located in the uveal canal in the eye and has subtypes depending on whether it develops in different parts of the eye. Desmoplastic melanoma is a type of melanoma consisting of spindle-shaped tumors. It is a rare variant of cutaneous

melanoma. Desmoplastic melanoma has been reported to generally occur on the skin of elderly individuals who are chronically exposed to sunlight [10].

2.5. Types of Non-Melanoma

Non-melanoma skin cancers are reported to be the most common malignancy among humans, with an incidence that has recently increased. The main reasons for this increase in the incidence rate are stated as exposure to UV radiation and increased exposure to sunlight as a result of depletion of the ozone layer. In addition, cumulative UV dose over many years is reported to be among the reasons for high incidence. 99% of non-melanoma skin cancer types are basal and squamous cell carcinomas. It has been reported in the literature that basal cell carcinoma predominates over squamous cell carcinomas. It has been reported that this dominance ratio varies between 1:1 and 10:1. As a result of research, it has been reported that basal cell skin cancer accounts for 80% of non-melanoma skin cancers. In addition, research has shown that it is difficult to distinguish basal cell skin cancer from squamous cell skin cancer, and therefore these two types of skin cancer are directly registered as non-melanoma skin cancer. The remaining 1% consists of Merkel cell, fat, adenocarcinoma and apocrine carcinomas and other rare types of carcinomas [11].

2.6. Diagnosis of Melanoma

Diagnostic methods of skin cancer are similar to diagnostic methods of other types of cancer. Clinical symptoms, imaging, physical examinations and laboratory examinations are among these methods. However, the most important and first method used when diagnosing melanoma is pathological examinations including immunohistochemical determinations. This pathological examination is of great importance to determine the stage, treatment and prognosis of melanoma [12].

There are different methods to diagnose the skin cancer, traditional and contemporary. Self-skin examination, optical coherence tomography, ultrasonography and dermoscopy [13].

2.6.1. Self-skin Examination

Self-skin examination (SSE) method is a simple detection method, but it has been stated that the rate of skin cancer detected by this method is between 6% and 50%. SSE is recommended

by the Australian Cancer Council and the American Academy of Dermatology. It has been stated that it is a cheap, easy and effective method because individuals can perform the SSE method on their own at home. It has also been stated that this method reduces the mortality rate of melanoma by up to 60% [13].

2.6.2. Dermoscopy

Dermoscopy method uses optical magnification to observe lesions on the skin. This method enables the examination of pigmented lesions in addition to the lesions detected by SSE [13].

2.6.3. Reflectance confocal microscopy (RCM)

Reflectance confocal microscopy (RCM) is another traditional diagnostic technique. It evaluates melanoma at the epidermis and papillary dermis level. In this technique, a low-power laser beam scans the sample tissue and measures the intensity of the emitted light. It creates contrasts in the image with the different reflection indices in the skin cells. RCM application is also a technique used to create algorithms and minor and major criteria in the diagnosis of melanoma. As a result of the research, it has been stated that the RCM technique has a sensitivity of over 90% in the diagnosis of melanoma [13].

2.6.4. High frequency ultrasonography

In the past years, ultrasound techniques have improved and enabled high-resolution images to be obtained in different pathological detections. The high resolutions obtained are helpful in visualizing skin layers and vessels in the diagnosis of melanoma. It has been stated that with this high resolution, there is a 99.4% correlation with pathology in melanoma scans. It has been stated that the presence of a solid, vascular and hypoechogenic structure as a result of ultrasound examinations indicates the presence of melanoma. Ultrasound techniques also have disadvantages in melanoma treatment. This disadvantage is that the distinction between melanoma and inflammatory infiltrates cannot be made correctly [13].

2.6.5. Optical coherence tomography

Optical coherence tomography (OCT) provides cross-sectional 2D and 3D images in melanoma treatment. OCT has been stated to be an effective method for imaging skin morphology and other areas. This method is only used to examine very small lesions [13].

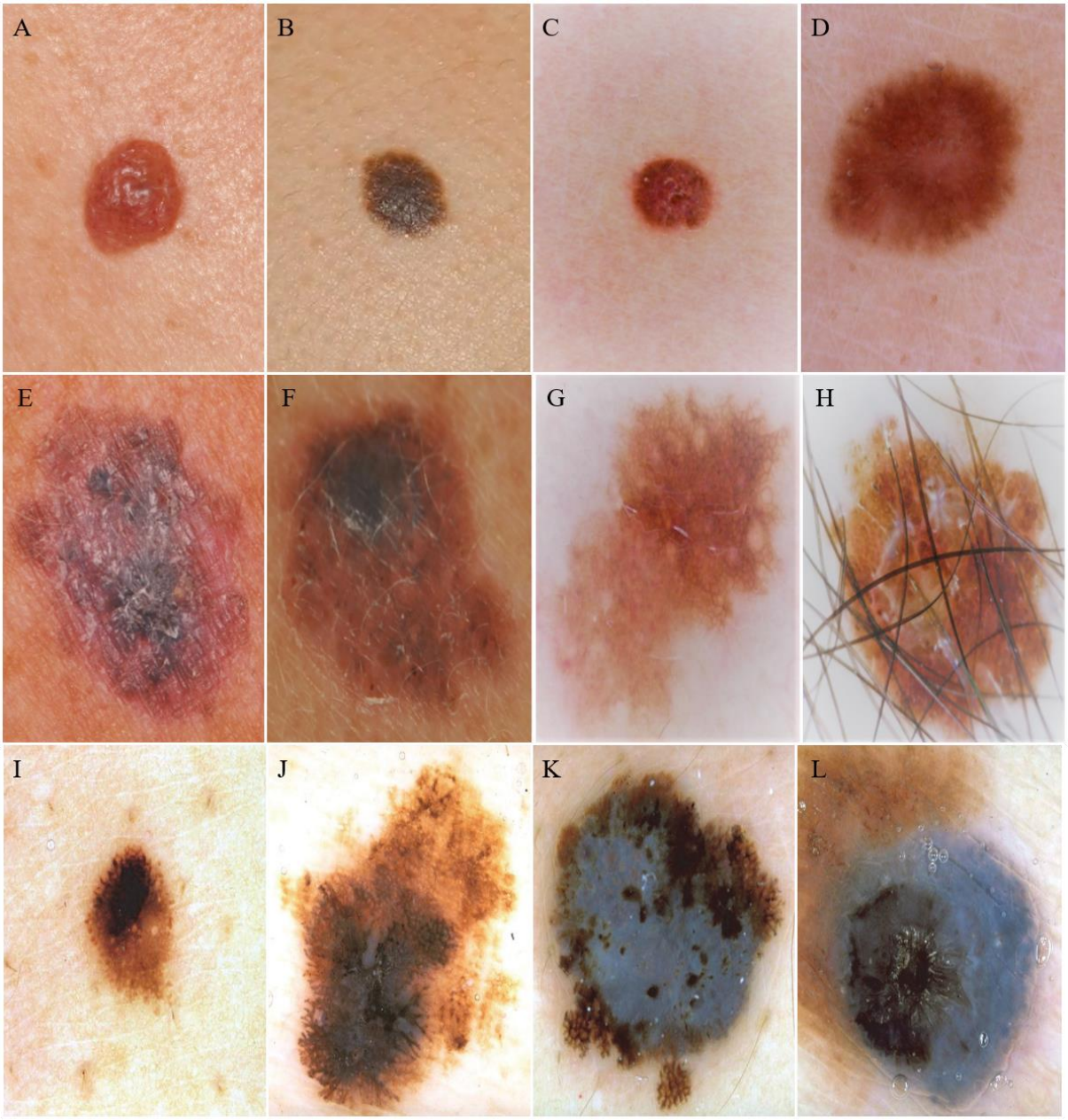

Figure 2.3. (A-D) images of benign melanoma, (E-F) dermatoscopic images of malignant melanoma and [14] (I-L), dermatoscopically obtained images of the stages of melanoma [5].

2.7. Treatment of Melanoma

There are certain treatment methods currently used in the treatment of melanoma. Surgery, radiotherapy, adjuvant, systemic and photodynamic treatments are among these methods. Surgical methods are the most common methods, biopsy and resection. Adjuvant treatment

for skin cancer is based on the patients' risk and clinical stage. It has been stated that there is currently a consensus that adjuvant treatment should be applied to low, medium and high-risk patients. However, it has also been stated that discussions continue about using this treatment method for very high-risk patients. Some type of melanoma must be treated individually and using different treatment methods. For example, adjuvant treatment along with interferon therapy is of great importance for high-risk patients. It has been stated that as a result of the lack of treatment and poor prognosis in skin cancer patients, other branches of medicine may also be involved in the treatment. In the study, they stated that recent developments in the fields of personalized and targeted treatment and immunotherapy have resulted in better results in patients with advanced stage skin cancer. In recent years, interest in the field of nanotechnology has increased intensely. Nanotechnology applications, especially in medicine, have increased and progress has been achieved in this field. In the application areas of nanotechnology in medicine, they mostly serve as drug or molecule carriers. Thanks to these carriers, improvements have been made in the field of drug distribution. Chemotherapy drugs do not specifically target cancer cells. It has been stated that as a side effect, they may cause various complications by affecting normal healthy cells in the body, and as a result, the patient's quality of life may be negatively affected. The field of nanotechnology provides assistance in delivering drugs to the target area. This benefit is provided by nanocarrier drug delivery systems, which serve to carry drugs and other active molecules to the targeted area. Compared to freely administered drugs, drugs administered with nanocarriers can affect specific areas. Thus, it is possible to reduce the potential side effects of drugs and increase the therapeutic effects. The important parameters in targeting rust are permeability and retention effects. Active targeting is seen as the aim of specifically recognizing, enhancing and targeting the tumor-antigen interaction by binding antibodies and peptides to the surface of drug delivery systems [12].

2.8. Drug Repositioning

It has been reported that drug discovery using traditional methods is a time-consuming process with high costs and risks. However, in recent years, the drug repositioning technique has become increasingly popular. Among the reasons why this method has attracted a lot of attention recently is that it is a low-risk, economical and highly efficient method compared to

classical methods. There are different approaches to drug repositioning studies: biological approaches, computational approaches and mixed approaches. These three approaches are frequently used in drug repositioning methods. Drug repositioning is the study of finding new and different uses of old drugs that are currently being used. Drug repositioning is seen as a very effective method in obtaining new purposes for the use of existing drugs. There are five steps to go through in traditional drug development processes. Discovery and preclinical studies of the drug, safety reviews, and FDA approval and post-market safety review. However, there are four stages to be passed in drug repositioning studies according to traditional methods. The first stage is compound identification. After the compound is identified, there are stages of acquiring and developing the compound. The last stage is to put it on the market by the FDA, which is common with traditional methods, and then examine the safety period. It has been reported that the rapid growth and development of bioinformatics information and big data in the field of biology and drug repositioning studies have significantly reduced the time spent on drug development studies. On average, it takes 1-2 years to determine new targets. However, it has been stated that it takes 8 years to obtain a repositioned drug. It has been previously noted that drug repositioning methods are low-cost. It has been stated that drugs produced by drug repositioning have a cost of 1.6 billion dollars, but drugs produced by traditional methods may have a cost of 12 billion dollars [15].

Drug repositioning does not focus on any structural modification of the drug. It deals with the current structure of the drug and the approved biological properties of this structure, at different doses and a new application area, or the immediate effects of the drug. These studies are based on two scientific foundations. The first of these foundations is the discovery of common biological points of some diseases as a result of human genome studies. The second basis is the study of the use of drugs developed for a specific disease outside of this disease. The second principle is also called the pleiotropic drug concept. As a result of recent studies, it has become possible to define diseases according to their molecular structures and to determine the similarities between them and other diseases and the degree of these similarities. Identifying the complex related elements between the disease-drug-target trio through in silico studies is one of the keys to drug repositioning. In line with this information, it has been stated that Parkinson's disease and Alzheimer's disease have 48 genes and 4

signaling pathways in common. In line with these common points, it has been reported that a certain drug may be effective against both diseases [16].

2.9. Drug Used in Chemotherapy

Chemotherapy is a type of treatment that aims to slow or stop the growth of cancer cells. These chemicals that target cancer cells also damage healthy cells. There are FDA-approved drugs released for chemotherapy treatment, such as Cobimetinib, Ipilimumab, Nivolumab, Trametinib, Vemurafenib, etc. [1].

2.9.1. Cobimetinib

Cobimetinib is a drug used to inhibit cell growth and reduce the proliferation of tumor cells. This drug is classified as a kinase inhibitor with antineoplastic activity and is a bioactive inhibitor. It inhibits mitogen-activated protein kinase. It inhibits MEK-1 catalytic activity [1].

2.9.2. Ipilimumab

The drug ipilimumab binds with T-lymphocyte-associated antigen 4. Antigen 4 is important in down-regulation of its expression in T cells in the immune system. As a result of this binding, the T-lymphocyte provides cytotoxic immune reactions and causes them to fight cancer cells as a result of the reaction [1].

2.9.3. Nivolumab

Nivolumab is a drug that has immune checkpoint inhibitors as well as antineoplastic activities. The drug acts directly on receptors on the cell surface. As a result of this effect, programmed cell death occurs, which is observed in many cancer cells. Tumor cells avoid the host's immune system by blocking this programmed cell death. This drug is generally used in combination with the drug Ipilimumab, which is intended to be used in melanoma treatments [1].

2.9.4. Trametinib

Trametinib is a cancer drug that also has antineoplastic activity. It is considered as an inhibitor of protein kinase activated by mitogens. Kinase activation such as ERK/RAS/RAF/MEK has a significant role in signaling pathways and cell growth regulation.

This agent is also called a kinase inhibitor. These inhibitors block the activities of abnormal proteins involved in the uncontrolled proliferation of cancer cells [1].

2.9.5. Vemurafenib

Researchers stated that the cells that make up 60% of melanoma cells are straightforward related to the Braf gene mutation. The drug vemurafenib is a kinase inhibitor. It is a BRAF inhibitor and has been reported to cause a decrease in the proliferation of cancer cells [1].

2.10. GSK2126458 (Omipalisib®)

The PI3K family consists of 15 lipid kinase enzymes that differ in their substrate properties, expression patterns, and modes of regulation. PI3Kalpha, one of these kinase enzymes, is an enzyme of high interest for cancer therapeutics. Knight and his colleagues reported the discovery of the compound GSK2126458 in their study. They stated that the compound GSK2126458 is an extremely potent and selective inhibitor of class 1 PI3K enzymes and mammalian target of rapamycin (mTOR). Knight et al also reported that the compound GSK2126458 had high mechanical and antiproliferative effects [17].

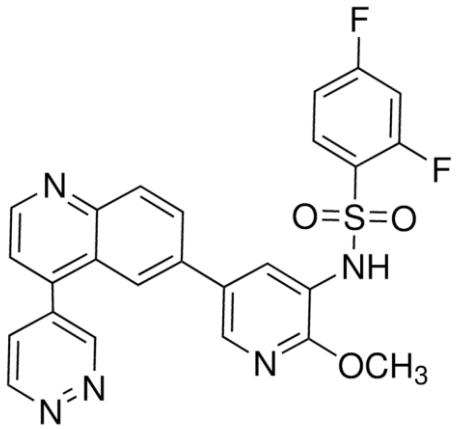

Figure 2.4. Chemical structure of GSK212458 (Omipalisib®) [18].

2.11. The Use of Nanotechnology for Melanoma

Nanotechnology is a field of study that attracts a lot of attention today and has high potential in the field of tissue engineering. Nanostructures have many important properties: large surface area/volume ratio, hydrophilicity, fiber diameter, stability, porosity. The most popular technique in the synthesis stages of these nanostructures is electrospinning. Electrospinning technique is the most widely used technique to produce nanofibers using natural and artificial polymers in tissue engineering and drug delivery applications [1].

The immune system does not attack normal cells in the body. Normal cells provide this if they do not cause any immune response in the immune system. The immune response is made through proteins. Melanoma cells also take advantage of not creating an immune response by using these proteins. However, any material or drug of extracellular origin inhibits these proteins and ensures the formation of an immune response. It has been reported that nanoparticles, nanofibers and biomaterials act as immunomodulators and the application of these materials can provide responses that cannot be achieved with traditional applications [19].

It has been stated that new strategies are needed in the treatment of a deadly disease such as skin cancer. The field of nanotechnology is a field that has established itself in the biomedical field. It has been stated that the field of nanotechnology provides carrier agents for drugs and other molecules in the treatment of melanoma [20].

Various methods are applied in the clinical treatment process of skin cancer. It has been stated that multi-target drugs are generally used in combination in order to increase drug effectiveness. However, nanotechnology-based drug delivery systems play an important role in skin cancer. The reason for this is that nanomaterials can overcome biological barriers in the body and provide drug delivery at the cellular level. Nanomaterial-assisted treatment studies in the treatment of skin cancer have recently attracted attention and been studied. As a result of these studies, nanomaterials can easily pass biological barriers due to their surface and size properties and shows cytotoxic cell effects specifically on melanoma cells. Another important point for nanomaterials and drug delivery systems is the reduction of toxicity and side effects outside the target tissue and thus increasing the effectiveness of drugs. Thus, it

has been stated that positive effects such as preventing the biodegradation of drugs administered to the patient outside the target area in the body, excretion of the drug from the body, and extending the half-life of the drug can be achieved with nanomaterials [12].

2.12. Electrospinning

The first and most important method preferred in nanofiber production is the electrospinning method. The electrospinning method has been stated to be simple, low-cost and high-efficiency. Because of these features, the electrospinning method is a method with high potential in biomedical fields and stands out among other methods. The electrospinning method is an electrohydrodynamic process in which polymer droplets are transformed into nano-sized fiber structures in an electric field. The electrospinning method consists of preparing the polymer solution to be electrospun, placing it in a syringe with a metal tip, creating an electric field between the syringe needle tip and the collector, and spraying the solution from the syringe tip to form nanofiber structures thanks to the electric field. As of today, natural and synthetic polymers have been used in nanofiber synthesis studies using the electrospinning method. With the advancement of nanofiber technology, nanofiber structures of different structures have been produced. By localizing drugs to the surface with single-layer nanofibers, burst drug release has become easier. Thanks to multilayer nanofibers, localization of drugs to the lower layers and controlled and continuous drug release are of interest in cancer treatment. Multilayer nanofibers enable synergistic treatment method by enabling multiple drug loading. Electrospinning is a method that allows the creation of continuous spindles from submicron to nanometer diameter. With this method, nanofibers with high surface area/volume ratio can be produced. In laboratory conditions, an electrospinning setup can be provided with a high voltage power supply, a flat tip needle tip, a syringe, a syringe pump and a conductive collector [21].

Electrospinning method has recently become an important technique to meet the production needs of nano and micro sized polymeric fibers. It has been stated that the electrospinning method is an excellent technique for producing fibers of all sizes using natural and synthetic polymers. It has been stated that electrospun fiber structures are currently used in many areas such as wound healing, tissue engineering, drug delivery systems and sensors. Nanofibers are

widely preferred in the biomedical field due to their large surface area, high drug loading capacity, strong mechanical properties and low cost [22].

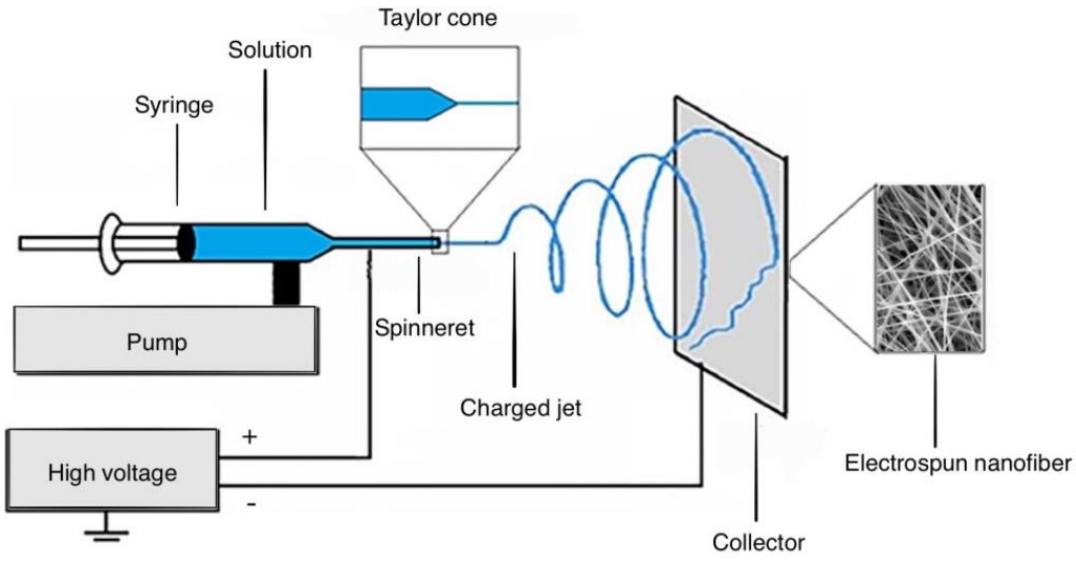

Figure 2.5. Basic electrospinning setup [23].

2.13. Melanoma Treatment Suggestions by Electrospun Fibers

In the study conducted by Zhu et al., shell-core nanofibers were produced by producing a shell loaded with chitosan and using PCL polymer and a core with PVP polymer loaded with 5-fluorouracil (5-FU). These nanofibers were produced for the purpose of being used in the treatment of melanoma skin cancer. It has been stated that the drug 5-FU has significant inhibitory effects on burst release, B16-F10 murine skin cancer cells. It has been stated that the continuous release of chitosan natural polymer has a healing effect on healthy cells after the negative effects of 5-FU drug [24].

In the study carried out by Sadeqzadeh et al., it was stated that the iron-doped nanocomposite nanofiber structures produced exhibited satisfactory mechanical properties. In addition, in vitro studies have shown that the nanofibers produced do not show high toxicity against melanoma cells and no significant side effects against normal cells. It has been stated that iron-doped nanocomposite nanofiber structures are intended to be used in cancer treatment and healthy tissue healing, depending on these properties [25].

Muthulakshimi and his colleagues stated that the use of nanofiber structures in drug delivery systems is promising for the future in cancer treatments. In this study, researchers loaded the extracts obtained from the *Terminalia catappa* plant into sodium alginate polymers. They obtained nanofiber structures by electrospinning. As a result of their later experiments, they stated that the material had antioxidant activity. In the cytotoxic activity results, it was stated that it had an inhibitory effect on B16-F10 cells. It has been reported that the materials produced in line with these results can be used in the treatment of skin cancer [26].

Serio and his colleagues, nanocomposite nanofibers were obtained using polyvinyl alcohol (PVA) and Gum Arabic. They stated that the use of these structures in cell culture did not have any side effects. Previous studies have stated that structures created using Gum Arabic and gold nanoparticles restrict the metastasis ability of metastatic skin cancer cells. As a result of these data, it was stated that nanocomposite nanofiber structures are a promising treatment for skin cancer [27].

In a study conducted by Garret et al., they loaded the drug imiquimod into PCL polymer in the treatment of surface basal cell carcinoma. As a result of this study, it was stated that adding the drug into this polymer provides faster drug release and better therapeutic results are obtained with fewer side effects with a smaller amount of drug [28].

2.14. Drug Delivery

Improved permeability and retention are the cornerstones of nanotechnology for the delivery of drugs to specific parts of the body. Lymphatic filtration is suppressed, making it possible for the molecules used to be delivered to malignant cells and retained at this point. Anatomically, having different pore sizes in vascularity also affects improved permeability and retention, as does the size, location, and type of tumor in the body [1].

Core-shell nanofiber structures can be given as examples of drug delivery systems with nanomaterials. Drug or active molecules can be incorporated into the core-shell structure. Depending on the structure of the material, biocompatibility, hydrophobicity and other mechanical properties may provide advantages in the treatment of skin cancer. In the study conducted by Zhu et al., core-shell nanofibers were produced and different drugs or active

molecules could be loaded into each layer of the nanofibers. In this way, improved therapeutic effects can be observed [24].

Among nanocarriers, nanofiber structures provide many advantages and it has been stated that successful results have been achieved in cancer treatments. Nanofibers are nanometer-sized thread-like structures produced using natural and synthetic polymers. Nanofibers are used in the treatment of many diseases other than cancer. It has been stated that nanofiber structures are frequently preferred structures in biomedical application areas due to their similarities to the extracellular matrix structure. The use of nanofiber structures has many desirable advantages in the field of treatment. Nanofiber structures have an easy production process. They are materials with high mechanical strengths. They have a high surface area/volume ratio. It has been stated that since they have a controlled drug release profile, they have the potential to minimize immediate effects in the body and the ability to maximize the drug effect by delivering the drug to the target area. Nanofiber structures have a large surface area/volume ratio and micro-sized pores, allowing direct interaction with drugs and active molecules. Thus, it has been stated that it increases drug encapsulation efficiency and drug loading efficiency. In addition, the fact that the production process of nanofibers can be manipulated allows nanofiber structures to specifically deliver the drug of choice. It has been stated that nanofiber structures can be used not only in the treatment of diseases but also in imaging stages for diagnosis of diseases [21].

2.15. PI3K-AKT-mTOR Relations with Melanoma

Phosphoinositide 3-kinase (PI3K) plays a critical role in the growth and transformation of cells. Mammalian target of rapamycin (mTOR) is a component of great importance in the PI3K pathway and is one of the central regulatory elements in cell growth. Protein kinase B (PKB), a serine/threonine protein kinase, is also known as Akt. PI3K/Akt/mTOR pathway is an intracellular signaling pathway involved in different cell functions. Its main functions are given as growth, apoptosis and proliferation. Additionally, this signaling pathway is among the signaling pathways most commonly activated in cancers [29].

PI3K-AKT is one of the pathways that has received the most attention in terms of study in the field of cancer. This pathway is a critical regulator of the physiological process of malignant

cells with aggressive behavior. Other studies in the literature have reported that the PI3K-AKT signaling pathway is a frequent target for genetic variations in different types of cancer. Since the PI3K-AKT pathway plays an active role in these areas, it has been accepted as a focal point in pharmacological studies. The PI3K-AKT pathway can be activated in numerous ways in melanoma. There are two different events that attract widespread attention in the literature. The first of these events is the activation of NRAS mutations, one of the oncogenes. The second event is that the tumor suppressor PTEN cannot be expressed or loses its function [30].

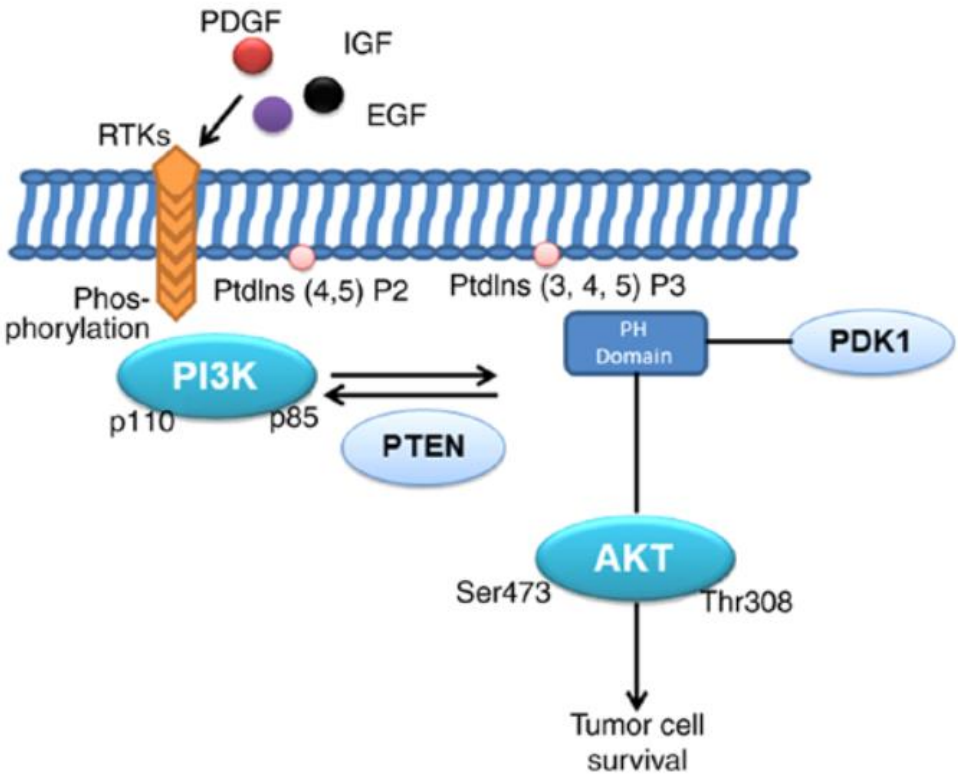

Figure 2.6. PI3K/AKT signaling pathway diagram. RTK recruits PI3K following activation and phosphorylation as a result of the uptake of growth factors. Also phosphorylates PtdIns (4,5) P2 to PtdIns (3,4,5) P3. As a result of this phosphorylation, AKT activation occurs as a result of PDK1 binding to the PH domain of AKT. Thus, all signaling pathways are activated and cell growth is regulated [31].

2.16. Polycaprolactone (PCL) and Polyvinylpyrrolidone (PVP)

Among the biodegradable synthetic polymers, PCL has received a lot of attention recently. PCL has become widely polymer in implanted biomaterials in many medical fields, including bone and cardiovascular tissue engineering, wound dressings, sutures, and nerve regeneration [32]. In addition, research has been carried out to provide controlled release of therapeutic molecules (for example, drugs, genes and proteins) by acting as carriers. PCL is a hydrophobic and slowly dissolving polymer. Although it is extensively used in the biomedical field. PCL is a polymer with many desirable properties, including good stability and easy processability, and is approved for use by the US Food and Drug Administration [32].

PCL and PVP are among the most popular polymers used. Having biodegradable structures, being hydrophilic, thermal and chemical stability are the most well-known features. These two polymers are widely used in controlled drug release technologies due to their tissue compatibility, easy electrospinning and solute permeability. PCL polymer is the polymer that provides strength in the structures, while PVP provides the necessary environment for drug release [33].

PVP is another example of biocompatible synthetic polymer. It is a very common polymer in biomedical applications because it is soluble in water and does not show toxic effects. PCL and PVP nanofibers have been widely used as blends in biomaterials. PCL-PVP nanofiber structures have been used in many studies. Suganya et al. [33], have a study in which they add medicinal plant extracts into PCL-PVP nanofibers for wound healing. Lee et al. [34], investigated the effects of PCL-PVP nanofiber structures on stem cells [35].

Zhu et al. [36], produced chitosan-loaded PCL shell and 5-fluorouracil-loaded PVP core nanofibers. Stating that they tried a new nanofiber delivery system for melanoma, they tested these nanofibers on B16-F10 and L929 cells. As a result of the study, they stated that the produced films stopped the cell cycle in the S phase and G2/M phase and prevented the proliferation of B16-F10 cells [36].

Nasari et al. [37], produced PCL/PVP core shell nanofibers, 5-fluorouracil loaded and containing multi-walled carbon nanotubes (MWCNTs) by electrospinning. They used MWCNT to increase the tensile strength of nanofibers whose mechanical properties decreased

with the increase in PVP amount. The results of MTT viability analysis performed on these materials indicated that the carrier material was not toxic but the drug loaded nanofiber structures had an effect on the cervical cancer cell line [37].

2.17. GSK2126458 and Cancer

Liu et al. [38], examined the effects of GSK2126458 PI3K inhibitor on the proliferation of nasopharyngeal carcinoma (NPC) cells. As a result of the study, it was stated that GSK2126458 PI3K inhibitor reduced the viability of NPC cells. They also stated that GSK2126458 inhibited the proliferation of NPC cells by affecting PI3K/Akt signaling pathways. Liu et al., who also examined the effects of GSK2126458 inhibitor on the migration of cells, stated that the migration of NPC cells was also inhibited. As a result of the study, Liu et al. stated that GSK2126458 inhibitor inhibited the proliferation and migration of NPC cells by suppressing PI3K/mTOR activity and also induced apoptosis and cell-cycle arrest in the cells [38].

In their study, Albawardi et al. [39] examined the effects of GSK2126458 inhibitor on different tumor types. As a result of GSK2126458 inhibitor applications, morphological changes, intracellular caspase-3 activity and immunohistochemical evidence of apoptosis were observed in invasive ductal carcinoma, morphological changes were observed in invasive lobular carcinoma tumor types, intracellular caspase-3 activity was observed in poorly differentiated signet ring adenocarcinoma of gastric origin, and immunohistochemical evidence of apoptosis was observed in adenocarcinoma of gastric origin. Additionally, no treatment effect was noted in ovarian serous carcinoma and moderately differentiated adenocarcinoma of colorectal origin [39].

In their study, Narov et al. examined the effectiveness of GSK2126458 PI3K/mTOR inhibitor in the treatment of kidney tumors in Tsc2+/- mice produced as a result of genetic engineering. As a result of the study, they stated that GSK2126458 inhibitor showed a significant decrease in the number and size of solid kidney tumors. Additionally, GSK2126458 inhibitor suppressed the proliferation of tumor cells and increased the apoptosis of solid tumors [40].

In their study, Park et al. [41] investigated the effect of GSK2126458 PI3K/mTOR inhibitor on the proliferation of human prostate cancer cells (PC3, DU145 and LNCaP). As a result of this application, it has been reported that GSK2126458 showed a significant anti-proliferative effect in these cell types with PTEN down regulation or loss of PTEN function. As a result of their studies, it was reported that anti-apoptotic Bcl-2 and Bcl-xl expressions also decreased as a result of studies conducted with the combination of GSK2126458 and AZD6244 inhibitors [41].

In their study, Basu et al. [42], investigated the effects of Omipalisib® (another name of GSK2126458) inhibitor using neurocutaneous melanocytosis (NCM) cells. As a result of their study, they stated that Omipalisib® prevented colony formation of cells and induced autophagic cell death [42].

3. MATERIALS AND METHODS

3.1. Materials

- 0.2, 15- and 50-mL Centrifuge Tubes
- 10-100 μL and 100-1000 μL micropipette tip
- 5-10 mL Serological Pipette
- 7-Hydroxy-3H-phenoxazin-3-one 10-oxide (Resazurin sodium salt)
- Beaker (50-250 mL)
- Chloroform ($CHCl_3$)
- Dichloromethane (DCM)
- Dimethyl sulfoxide (DMSO)
- Dimethylformamide (DMF)
- Dulbecco's Modified Eagle's Medium (DMEM) – High Glucose
- Fetal Bovine Serum (FBS)
- GSK2126458 (Omipalisib®)
- Methanol (CH_3OH)
- Micropipette
- Phosphate Buffer Solution (PBS)
- Polycaprolactone (PCL)
- Polyvinylpyrrolidone (PVP)
- Tetrahydrofuran (THF)

3.2. Methods

3.2.1. Production of GSK2126458 Loaded and Non-Loaded PCL/PVP Nanofibers

The polymer, solvent and ratios used for nanofiber production by electrospinning are given in Table 3.1.

Table 3.1. Table of polymers, solvents and ratios prepared for electrospin.

Solvent		**Chloroform:Methanol (5 mL)**		**DCM:DMF (5 mL)**
Ratio		4:1	3:1	1:1
Amount of polymer (g)	**PCL (Avg. MW: 80,000)**	0.35	0.35	0.575
	PVP (Avg. MW:10,000)	0.15	0.15	0.025
	PVP (M_r 1,100,000.00)	0.15	0.15	0.025

Avg. MW: Average molecular weight, M_r: Relative formula mass

All polymer solutions used for electrospinning were prepared as PCL/PVP mixture. As the first solution, PCL (Avg. MW: 80,000) and PVP (Avg. MW: 10,000) were dissolved in Chloroform:Methanol (3:1). Then, the Chloroform:Methanol ratio was changed to 4:1. In the following solutions, PVP (M_r: 1,100,000.00) was used instead of PVP (Avg. MW: 10,000). Different solutions were prepared with new PVP as Chloroform:Methanol (3:1), Chloroform:Methanol (4:1) and DCM:DMF (1:1). Each solution was stirred with a magnetic stirrer at room temperature for 24 hours. At the end of 24 hours, the solutions were taken into a 5 mL syringe. The syringe needle tip was flattened with sandpaper and a blunt end was obtained. The solutions were electrospun to test different electrospinning conditions.

After the optimizations for solution and electrospinning conditions for nanofiber production were completed, drug-containing nanofiber production was started. PCL/PVP polymers were dissolved in DCM:DMF (1:1). After the polymers were completely dissolved in the solvent at room temperature with a magnetic stirrer, different amounts of drug solution were added to the polymer solutions in the form of droplets.

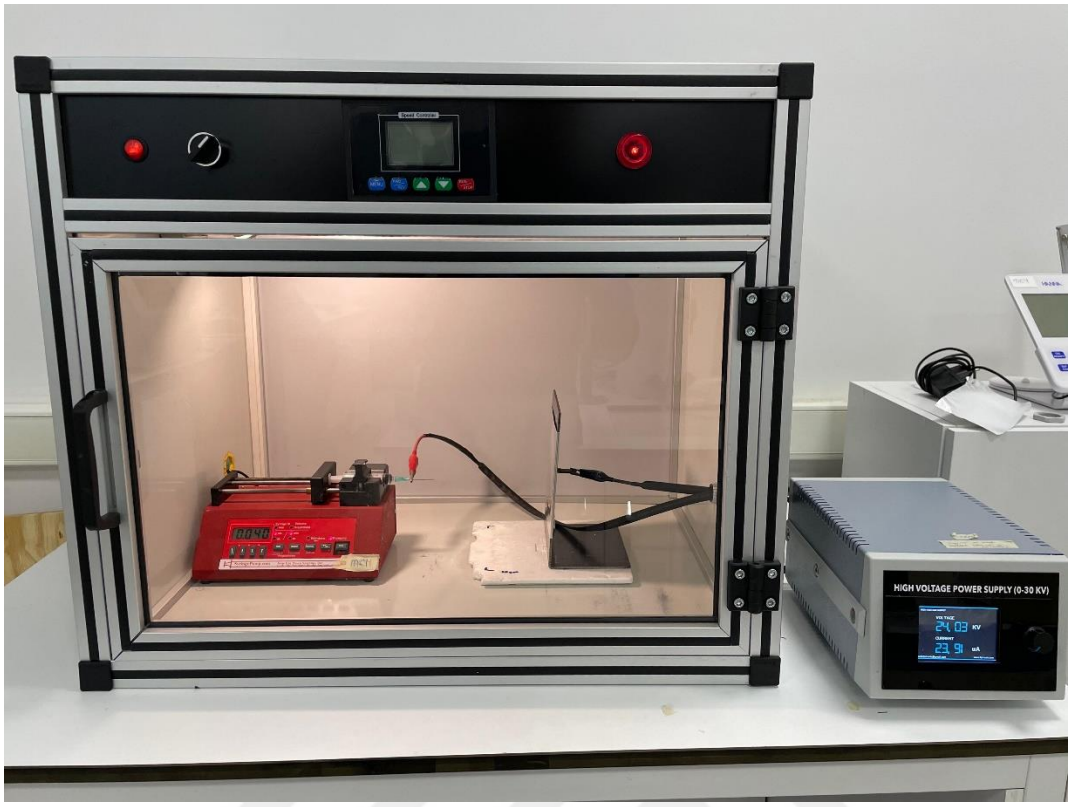

Figure 3.1. Image of the electrospinning device (Fytronix, Türkiye) used in electrospun nanofiber production.

3.2.2. Characterization of GSK2126458 Loaded PCL/PVP Nanofibers

Morphology of nanofiber structures observed by Scanning Electron Microscope (SEM) analysis (FEI, Quanta 650 Field Emission SEM). ImageJ ((National Institute of Health, MD) software was used to determine fiber diameters and their distribution from SEM images. Confirmation of loading of GSK2126458 into PCL/PVP nanofiber structures confirmed by fourier transmission infrared (FTIR) spectrometry (Bruker, VERTEX 70v) [35], [4]. Hydrophilicity of the membranes ($n=3$) determined by contact angle measurement (Attension Theta Flex) using the plate method. The mechanical properties of the membranes investigated using tissue analyzer Stable Microsystems (Model TA.XTPlus, SurreyEngland).

3.2.3. Cell Culture Studies

3.2.3.1. Cell Seeding and Viability Assay

In this study, B16-F10 mouse melanoma cell line (ATCC: CRL-6475^{TM}) was used in cell culture studies. B16-F10 cell line was cultured in DMEM-HG medium containing 10% FBS, 1% Penicillin/Streptomycin and 1% L-Glutamine.

To determine the IC_{50} for GSK2126458 drug on B16-F10 melanoma cells, 10,000 cells per well were seeded in 96-well plates in 200 µL of cell growth medium. First, drug concentrations between 0-50 µM were prepared in cell growth medium to determine the IC_{50} value. The IC50 value is the half-maximal inhibitory concentration of a substance that inhibits a biochemical or biological event. At the end of 24 hours, the medium of the confluent cells was replaced with 100 µL of medium containing the drug and cultured for 24 hours. At the end of 24 hours, the cell growth medium was replaced with DMEM-HG media containing 10% resazurin, 1% L-Glutamine and 1% P/S and waited for 2-3 hours for cells metabolic activity and color change on media. After incubation time, measurements were taken at wavelengths of 570-600 nm with a UV-vis spectrophotometer (BMG LabTech, SPECTROstar® Nano).

Electrospun GSK2126458/PCL/PVP membranes were cut to size appropriate for the 24-well plate wells 1.5 cm in diameter. Sterilization of membranes was achieved with UV light under sterile conditions. UV light applied for 1 hour to each side of membranes. Previously sterilized stainless-steel rings were placed on top of the membranes that placed in the wells. 50 µL of DMEM-HG cell medium containing 100,000 cells were added onto the membranes in a small diameter. The cells were then cultured in a 5% CO_2 incubator at 37°C for 1 hour to allow the cells to attach to the surface of the membranes. 950 µL of cell culture medium was added onto the cell seeded membranes after 1 hour culture. Cell seeded membranes were cultured at 37°C in 5% CO_2 incubator for 2 days. Resazurin analysis was applied to the cell to determine cell viability after 24 h and 48 h culture as described in the previous paragraph.

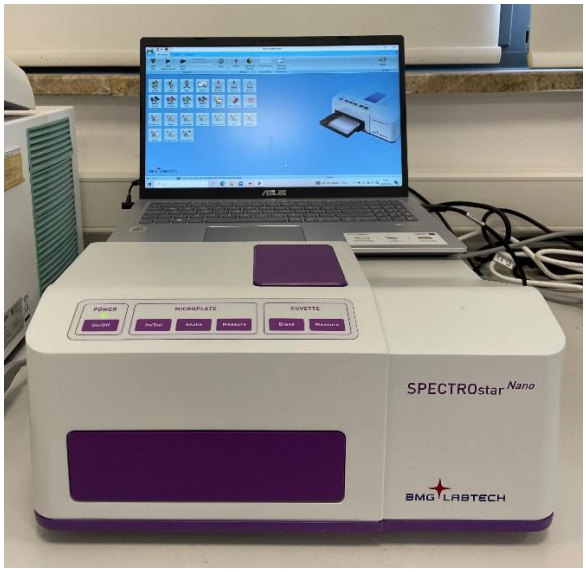

Figure 3.2. Image of UV-vis spectrophotometer device used in the analysis.

3.2.3.2. Visualization of Cell Morphology with SEM

Cell adhesion to membranes was determined by SEM analysis. For SEM analysis of the cells, culture medium on the membranes was removed and membranes were washed 2 times with PBS. 200 µL/well of 2.5% (v/v) glutaraldehyde solution in PBS was applied to the membranes and left at room temperature for 30 minutes. At the end of the period, the membranes were washed twice with PBS. After the cells were fixed, they were kept in ethanol solutions of different concentrations (30%, 50%, 70%, 90% and 100%) or 2 minutes for dehydration. The membranes were then completely dried in 100% hexamethyldisilazane (HMDS) for 5 minutes. After removing HMDS, the membranes were waited under fume hood for one night. Gold coated membranes were analyzed by SEM at 10 kV under vacuum.

3.2.3.3. Immunofluorescent Staining

Immunofluorescence staining was carried out to show the morphology of the cell nucleus and fibrous actin protein distribution in the cell cytoplasm. Used cell medium on the membranes was removed and the membranes were washed 3 times in PBS. Fixation was caried out with 2.5% (v/v) glutaraldehyde for 20 minutes and then membranes washed 3 times in PBS. At the end of the period, the membranes were kept in 0.1% (v/v) Triton X-100 solution for 10 minutes. Triton X-100 solution was removed and membranes were washed 3 times with PBS.

At the end of washing, DAPI (4', 6-diamidino-2-feniliindol dihydrochloride) (1:1000 v/v) and anti F-actin (alexa fluor 488 reagent) (1:100 v/v) solution diluted in PBS containing 1% (w/v) bovine serum albumin (BSA) protein was added to the membranes and waited for 30 minutes. At the end of the period, the membranes were washed 3 times with PBS and imaged under inverted phase contrast microscope with fluorescent attachment (Leica).

3.2.4. Antibacterial Analyzes

Two methods were used to evaluate the antibacterial activities of GSK2126458-loaded PCL/PVP membranes. Agar diffusion method (semi-quantitative) was used as the first method. For this, 0.5 McFarland bacteria concentration was prepared in PBS and inoculated on nutrient agar (NA) by the spreading method. UV sterilized membranes, were cut into 10 mm in diameter, they were placed on the seeded agars and incubated at 37°C for 24 hours. Antibacterial activity was evaluated by measuring the diameter of the inhibition zones.

The second method used to evaluate antibacterial activity is the ''Shake Flask Method''. The membranes were weighed as 0.2 g and both sides were exposed to UV sterilization for 30 minutes. Membranes without drug loading were used as negative control in the experiment. In this method, 100 µL of 0.5 McFarland bacterial suspension (10^8 CFU/mL) was mixed with 900 µL ''nutrient broth'' and 9 mL of PBS in each sterile test tube and the bacteria concentration was adjusted to 10^6 CFU/mL in the final solution. Pre-sterilized 0.2 g membranes were placed in 10^6 CFU/mL bacterial suspension and incubated at 37°C for 24 hours with shaking at 200 rpm. At the end of 24 hours, colony numbers were counted and antimicrobial activity was calculated as %reduction using the equation below. A and B are the number of colonies detected from the negative control and processed samples, respectively [43]. The microorganisms used in the experiments are as follows; *Escherichia coli, Staphylococcus aureus, Pseudomonas aeruginosa* and Methicillin-resistant *Staphylococcus aureus* (MRSA).

$$Cell\ growth\ inhibition(\%) = \frac{A - B}{A} * 100$$

3.2.5. Statistical Analyzes

“Graph-Pad Prism’’ (version 10.2.3, USA) program was used for statistical analysis. One-way ANOVA test was applied to determine the significant differences between the groups and “Tukey-Kramer multiple comparisons test’’ was applied as a “post Hoc test”

4. ANALYSIS AND DISCUSSION

4.1. Preparation of PCL Membranes

PCL/PVP fiber structures to be used in cell culture were electrospun onto PCL membrane. 10 g of PCL was dissolved in 100 mL of THF and stirred with a magnetic stirrer for 24 hours. After 24 hours, the completely dissolved 10% (w/v) PCL solution was distributed to 7 cm diameter glass Petri dishes as 3 mL. The tops of the glass Petri dishes were covered with perforated aluminum foil and the THF solvent was allowed to evaporate in a fume hood for at least 3 days. Thus, thin and flat PCL membranes were obtained.

4.2. Production and Optimization of Drug-Loaded PCL/PVP Fiber Membranes

Many different conditions were tried to obtain smooth PCL/PVP fibers as beading free and non-wavy morphology. The first condition was determined as 10% total polymer content in 5 mL of chloroform/methanol (4:1). 0.35 g of PCL (Avg. Mn: 80,000) and 0.15 g of PVP (Avg. MW: 10,000) were dissolved in 4 mL of chloroform and 1 mL of methanol. The solution was stirred with a magnetic stirrer at room temperature for 24 h. The needle tip of the 5 mL syringe was flattened with sandpaper. The solution was taken into the syringe and electrospinning was attempted. However, the viscosity of the solution was observed to be high and electrospinning attempts did not yield results. For this reason, PVP (M_r: 1,100,000.00) was selected to prepare the PCL/PVP solution and all solutions were prepared with this PVP.

Table 4.1. Condition and solvent table of fiber structures provided by electrospinning method.

Electrospin Condition	Solvents				
	Chloroform	**Methanol**	**DCM**	**DMF**	
10 cm 15 kV 0.700 mL/h PCL/PVP 10%	•	•			Chloroform/ Methanol (4:1)
10 cm 15 kV 0.750 mL/h PCL/PVP 10%	•	•			
10 cm 18 kV 0.750 mL/h PCL/PVP 10%	•	•			
10 cm 15 kV 0.800 mL/h PCL/PVP 10%	•	•			
10 cm 15 kV 0.750 mL/h PCL/PVP (70:30) 10%	•	•			Chloroform/Methanol (3:1)
12 cm 15 kV 0.750 mL/h PCL/PVP (70:30) 10%	•	•			
8 cm 15 kV 0.750 mL/h PCL/PVP (70:30) 12%	•	•			
10 cm 15 kV 0.750 mL/h PCL/PVP (70:30) 12%	•	•			
10 cm 17 kV 0.750 mL/h PCL/PVP (70:30) 12%	•	•			
12 cm 15 kV 0.750 mL/h PCL/PVP (70:30) 12%	•	•			
10 cm 15 kV 0.750 mL/h PCL/PVP (70:30) 14%	•	•			
10 cm 17 kV 0.750 mL/h PCL/PVP (70:30) 14%	•	•			
10 cm 20 kV 0.750 mL/h PCL/PVP (70:30) 14%	•	•			
10 cm 15 kV 0.750 mL/h PCL/PVP (70:30) 15%	•	•			
10 cm 17 kV 0.750 mL/h PCL/PVP (70:30) 15%	•	•			
15 cm 24 kV 0.02 mL/min. 10% PCL 2% PVP			•	•	DCM/DMF (1:1)
15 cm 24 kV 0.02 mL/min. 12% PCL 0% PVP			•	•	
15 cm 24 kV 0.03 mL/min. 10% PCL 2% PVP			•	•	
15 cm 24 kV 0.03 mL/min. 12% PCL 0% PVP			•	•	
15 cm 24 kV 0.04 mL/min. 10% PCL 2% PVP			•	•	
15 cm 24 kV 0.04 mL/min. 12% PCL 0% PVP			•	•	
15 cm 24 kV 0.04 mL/min 11.5% PCL 0.5% PVP			✓	✓	

PCL (Avg. MW: 80,000), **PVP** (Mr 1,100,000.00)

- **:** Tested conditions, ✓ : Selected condition

To produce drug-loaded PCL/PVP electrospin fiber structures, polymers dissolved in 11.5% (w/v) PCL and 0.5% (w/v) PVP, in 5 mL DCM/DMF (1:1). Phase contrast images of the fibers produced according to the electrospinning conditions given in Table 4.1. were obtained by light microscopy.

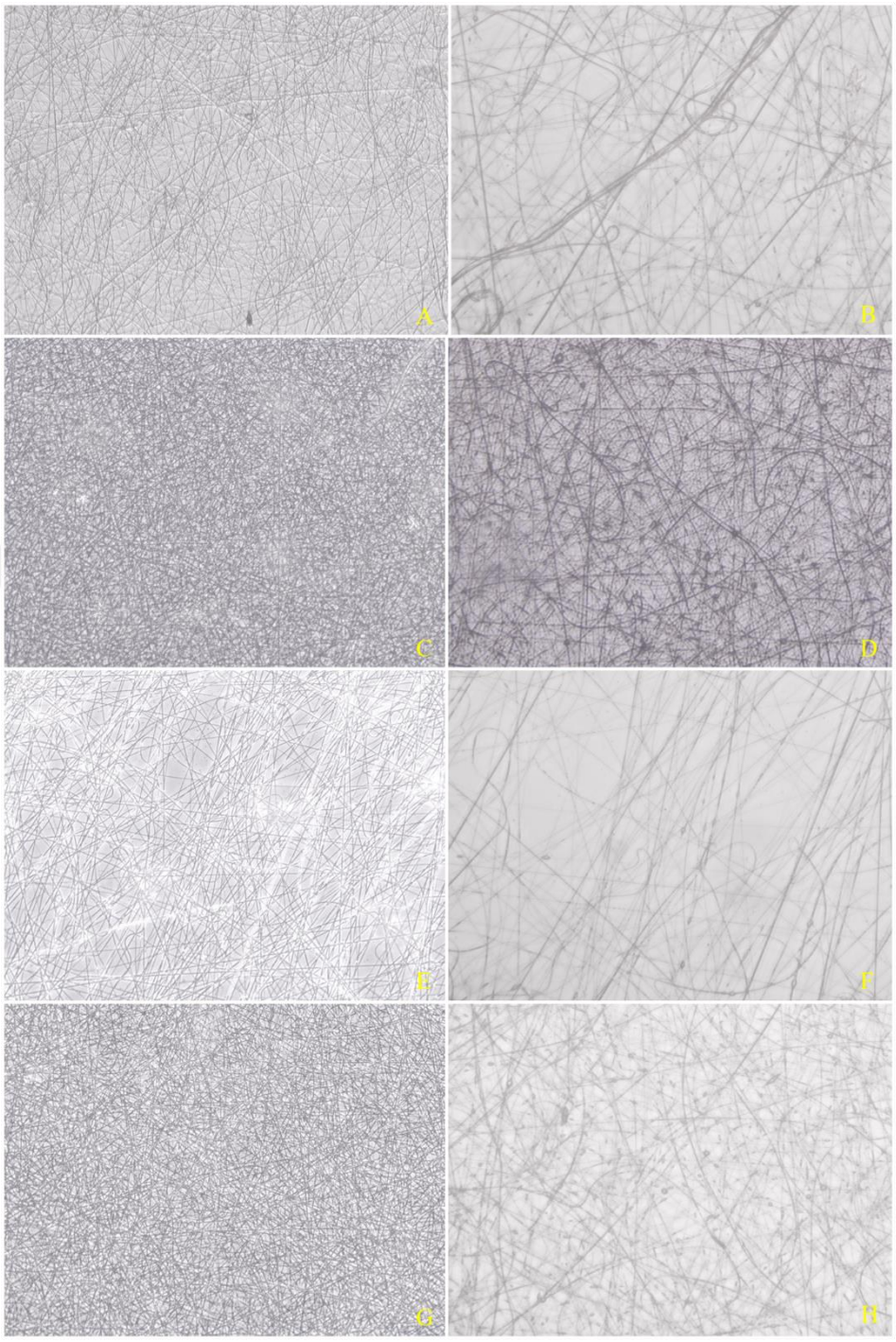

Figure 4.1. Phase contrast images of fibers obtained by light microscopy. 10 cm 15 kV 0.7 mL/h PCL/PVP (10%) Chloroform/Methanol (4:1) (A-B), 10 cm 15 kV0.75 mL/h PCL/PVP (10%) Chloroform/Methanol (4:1) (C-D), 10 cm 18 kV 0.75 mL/h PCL/PVP (10%) Chloroform/Methanol (4:1) (E-F) and 10 cm 15 kV 0.8 mL/h PCL/PVP (10%) (G-H) Chloroform/Methanol (4:1), A-C-E-G 10X and B-D-F-H 20X.

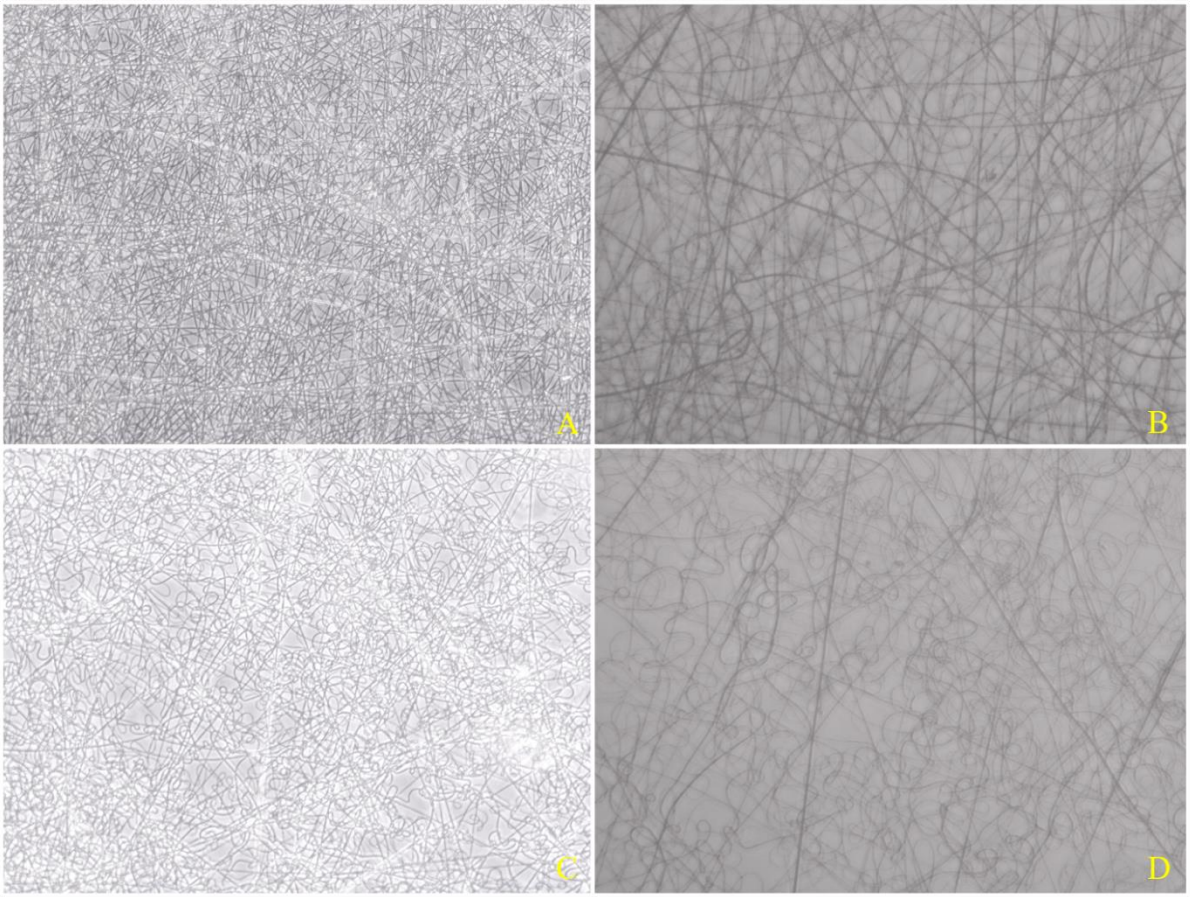

Figure 4.2. Phase contrast images of fibers obtained by light microscopy. 10 cm 15 kV 0.75 mL/h PCL/PVP (70:30) (10%) Chloroform/Methanol (3:1) (A-B), 12 cm 15 kV 0.75 mL/h PCL/PVP (70:30) (10%) Chloroform/Methanol (3:1) (C-D), A-C 10X and B-D 20X.

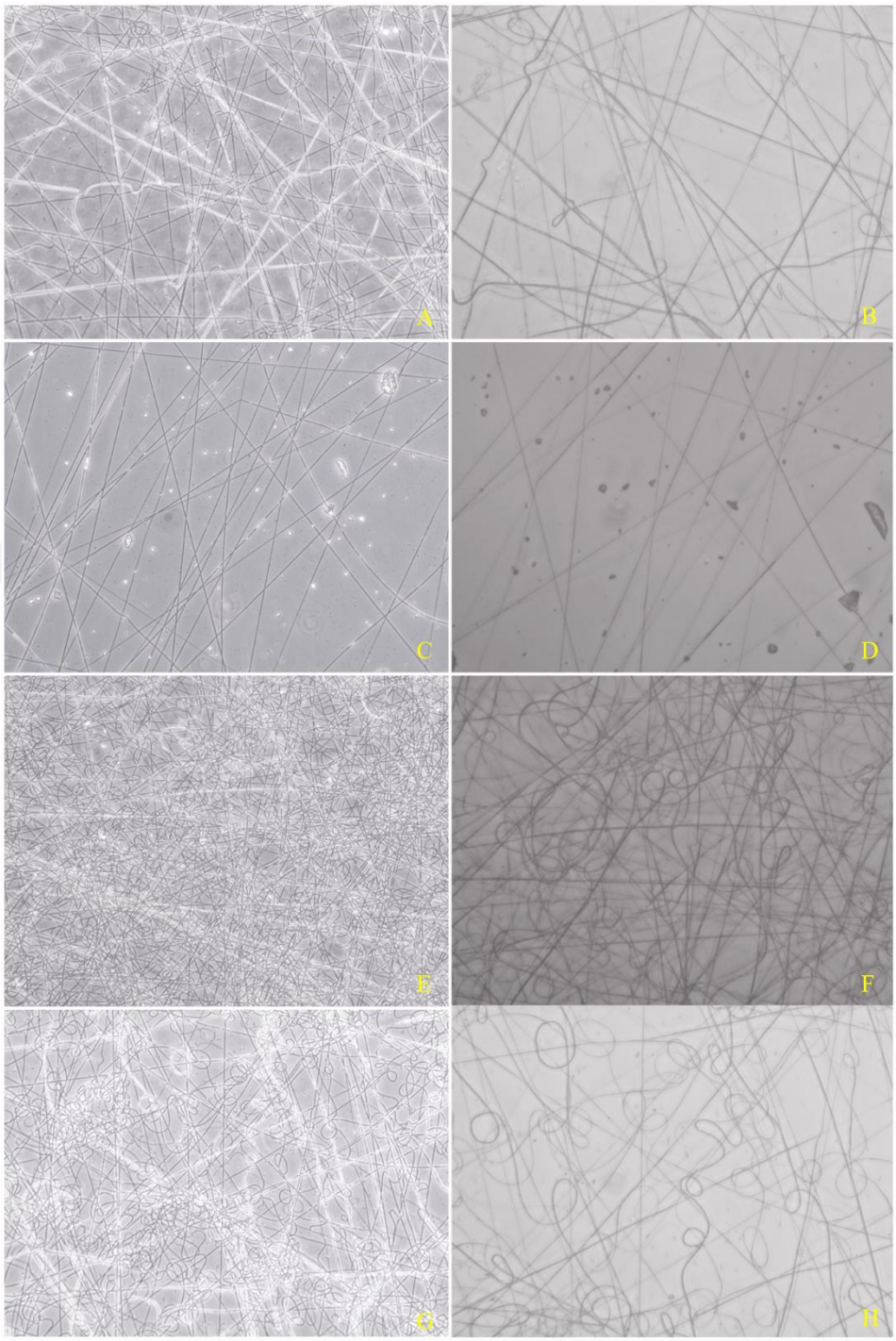

Figure 4.3. Phase contrast images of fibers obtained by light microscopy. 8 cm 15 kV 0.75 mL/h PCL/PVP (70:30) (12%) Chloroform/Methanol (3:1) (A-B), 10 cm 15 kV 0.75 mL/h PCL/PVP (70:30) (12%) Chloroform/Methanol (3:1) (C-D), 10 cm 17 kV 0.75 mL/h PCL/PVP (70:30) (12%) Chloroform/Methanol (3:1) (E-F) and 12 cm 15 kV 0.75 mL/h PCL/PVP (70:30) (12%) (G-H) , A-C-E-G 10X and B-D-F-H 20X.

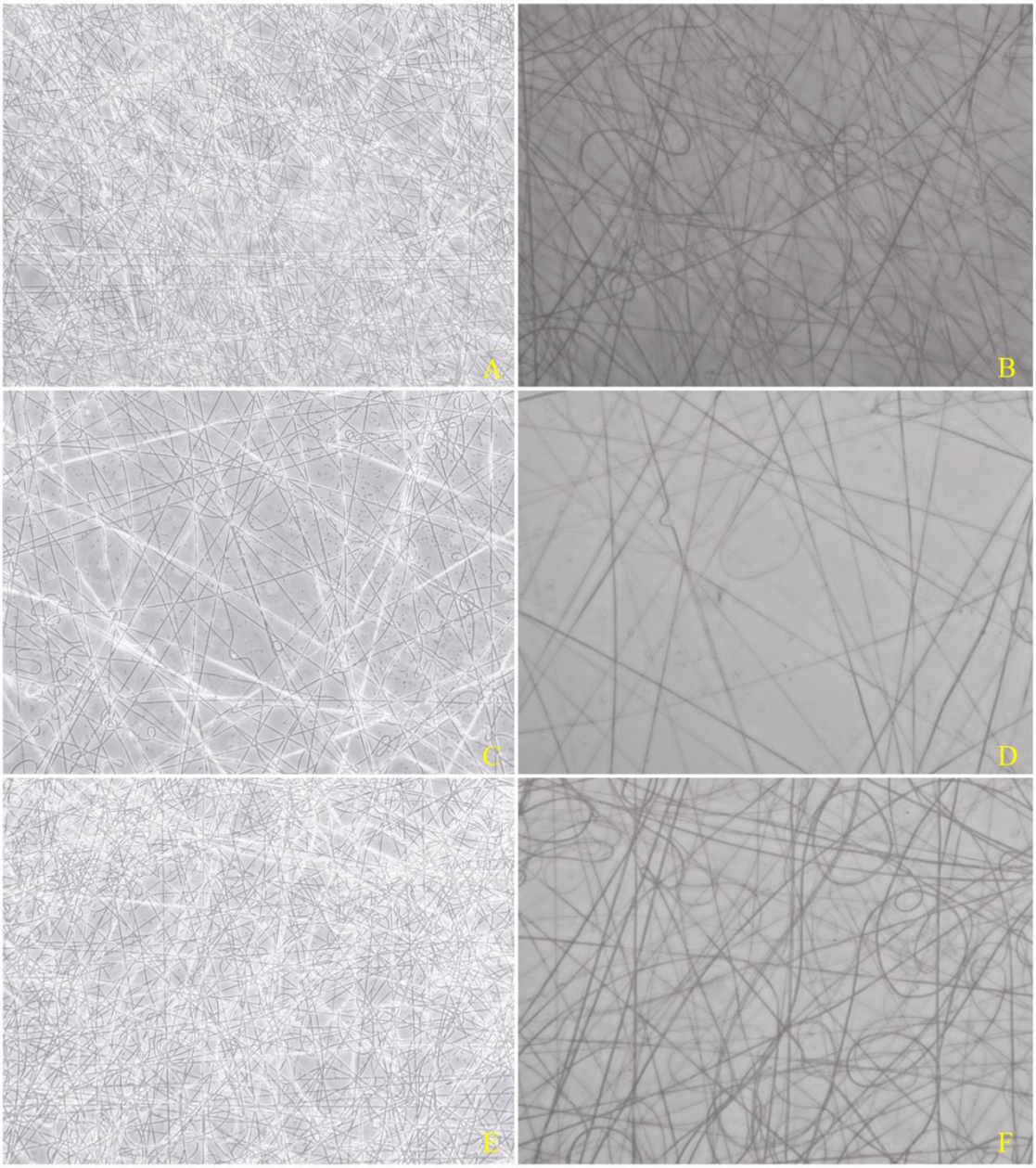

Figure 4.4. Phase contrast images of fibers obtained by light microscopy. 10 cm 15 kV 0.75 mL/h PCL/PVP (70:30) (14%) Chloroform/Methanol (3:1) (A-B), 10 cm 17 kV 0.75 mL/h PCL/PVP (70:30) (14%) Chloroform/Methanol (3:1) (C-D), 10 cm 20 kV 0.75 mL/h PCL/PVP (70:30) (14%) Chloroform/Methanol (3:1) (E-F) , A-C-E-G 10X and B-D-F-H 20X.

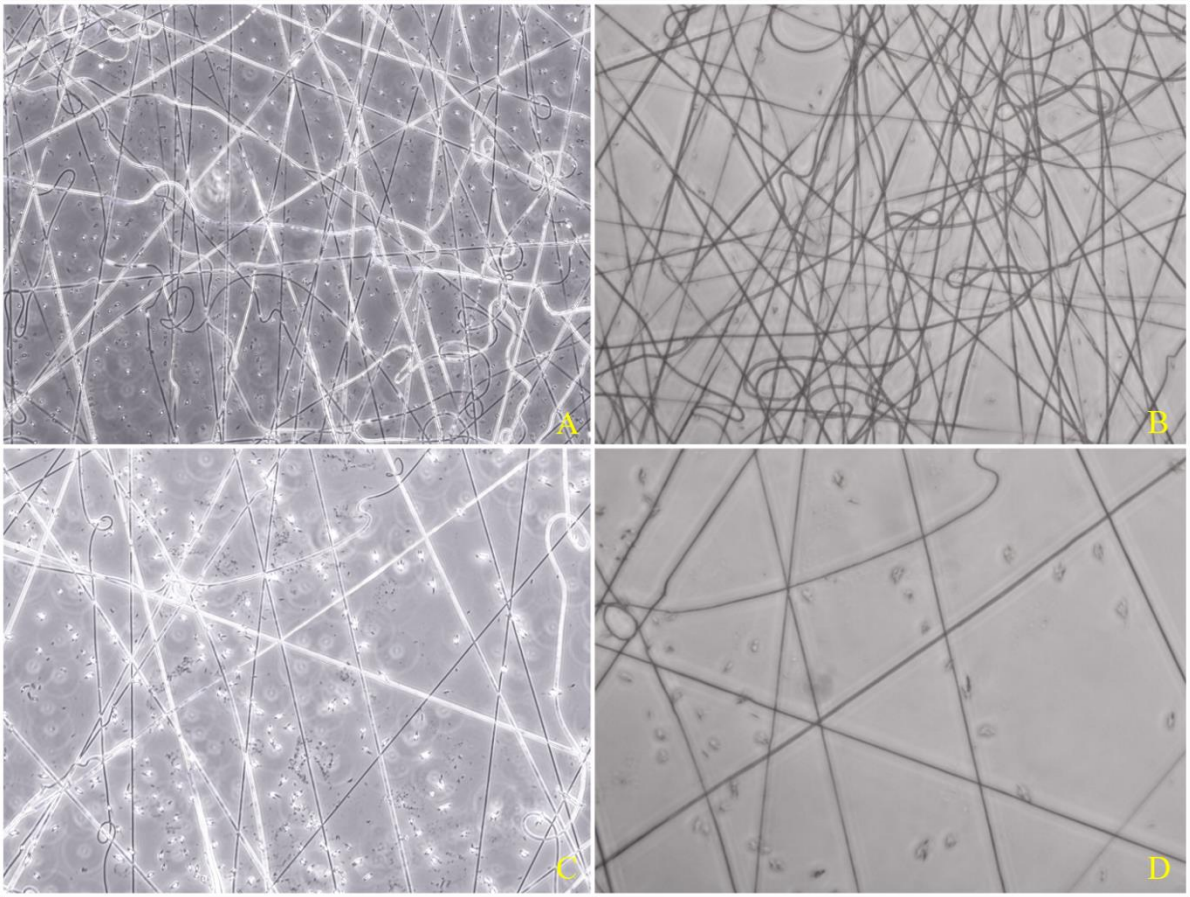

Figure 4.5. Phase contrast images of fibers obtained by light microscopy. 10 cm 15 kV 0.75 mL/h PCL/PVP (70:30) (15%) Chloroform/Methanol (3:1) (A-B), 10 cm 17 kV 0.75 mL/h PCL/PVP (70:30) (15%) Chloroform/Methanol (3:1) (C-D), A-C 10X and B-D 20X.

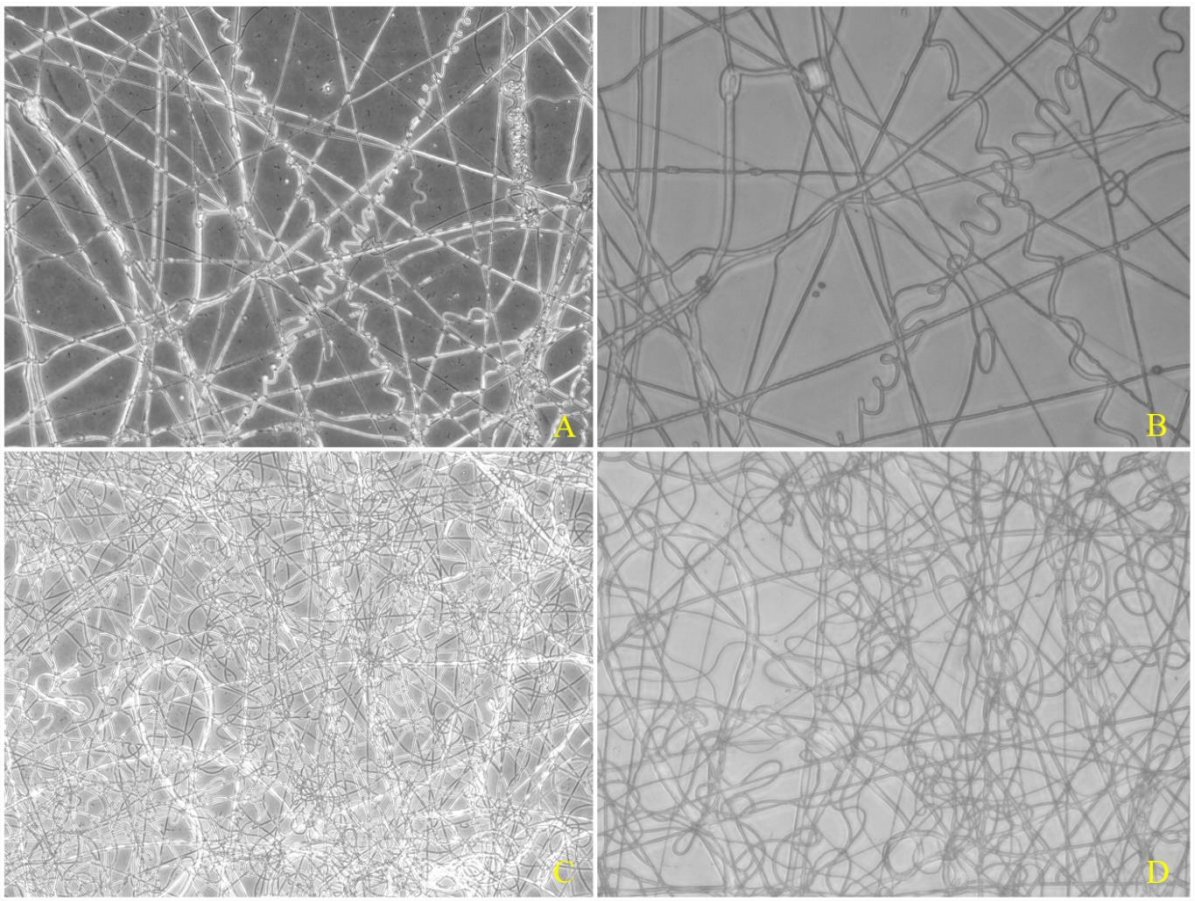

Figure 4.6. Phase contrast images of fibers obtained by light microscopy. 15 cm 24 kV 0.02 mL/min PCL/PVP (10%-2%) (12%) DCM/DMF (1:1) (A-B), 15 cm 24 kV 0.02 mL/min PCL/PVP (12%-0%) (12%) DCM/DMF (1:1) (C-D), A-C 10X and B-D 20X.

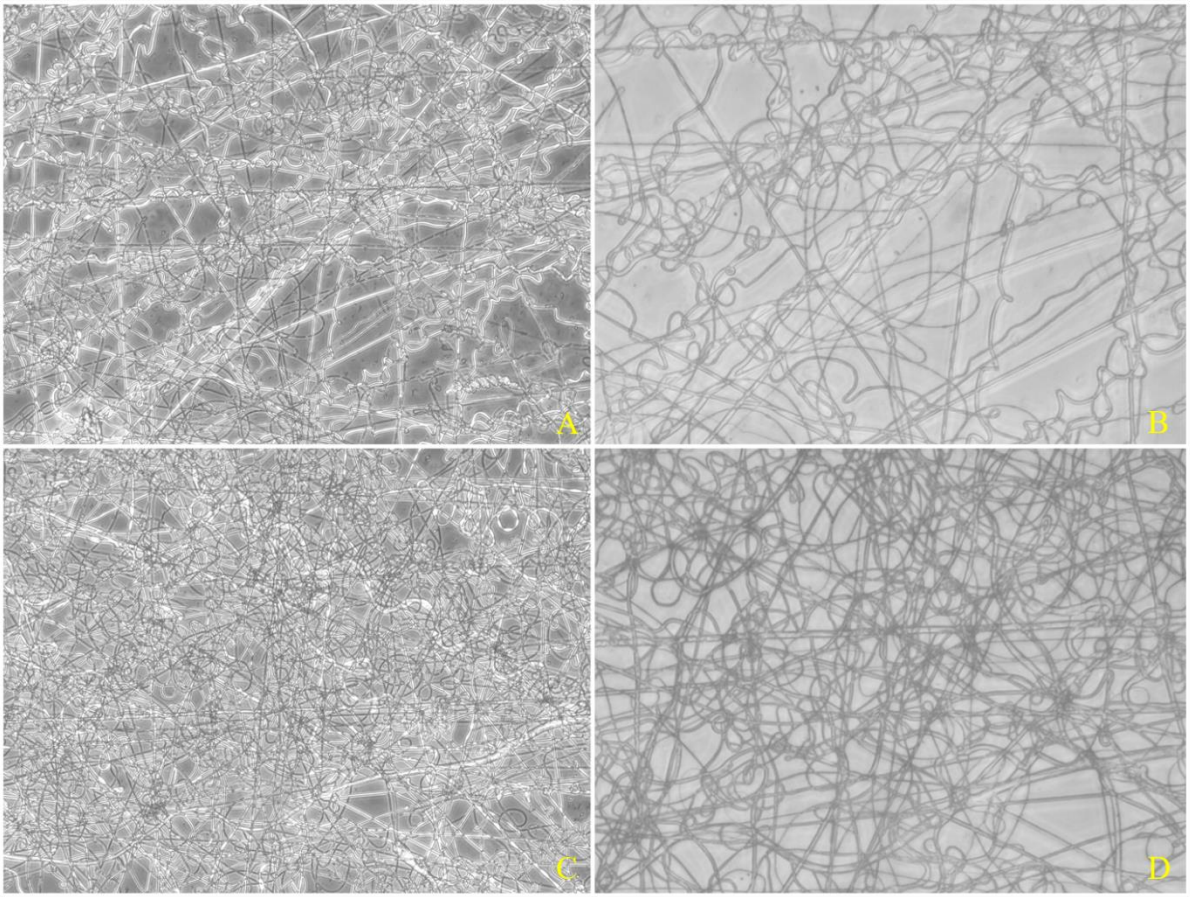

Figure 4.7. Phase contrast images of fibers obtained by light microscopy. 15 cm 24 kV 0.03 mL/min PCL/PVP (10%-2%) (12%) DCM/DMF (1:1) (A-B), 15 cm 24 kV 0.03 mL/min PCL/PVP (12%-0%) (12%) DCM/DMF (1:1) (C-D), A-C 10X and B-D 20X.

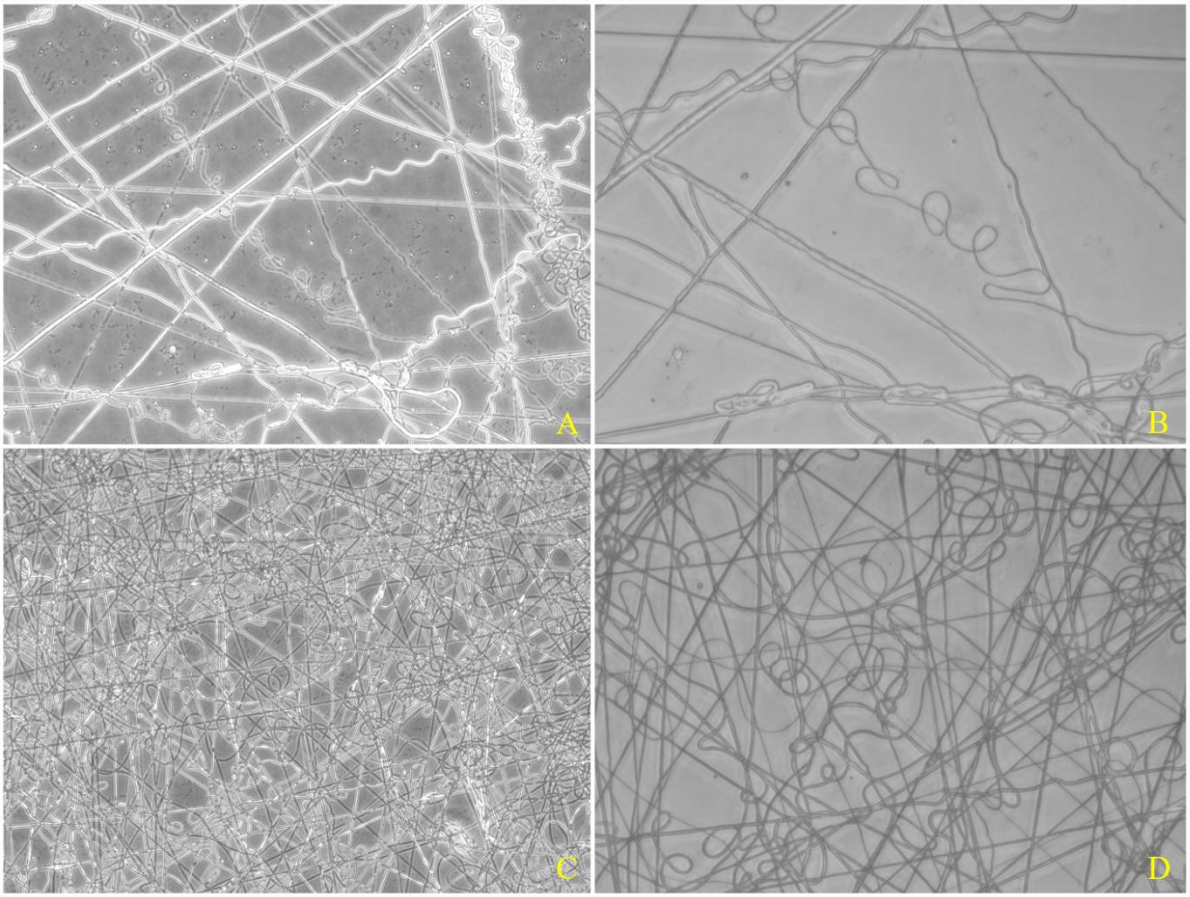

Figure 4.8. Phase contrast images of fibers obtained by light microscopy. 15 cm 24 kV 0.04 mL/min PCL/PVP (10%-2%) (12%) DCM/DMF (1:1) (A-B), 15 cm 24 kV 0.04 mL/min PCL/PVP (12%-0%) (12%) DCM/DMF (1:1) (C-D), A-C 10X and B-D 20X.

To produce drug-loaded PCL/PVP electrospin fiber structures, polymers dissolved in 11.5% (w/v) PCL and 0.5% (w/v) PVP, in 5 mL DCM/DMF (1:1) [44]. After the PCL/PVP solution was obtained 10 mM GSK2126458 added to this solution at different amounts (Table 3) and then waited for 24 hours for the polymers to dissolve in the solvent to obtain a homogenous solution. DMSO concentration was kept constant for all samples.

Table 4.2. Table of GSK2126458 and DMSO amounts contained in sample group.

	Volume (µL)	
Sample Groups	**GSK2126458 (10mM)**	**DMSO**
PCL/PVP/Control	0	100
PCL/PVP/50	50	50
PCL/PVP/75	75	25
PCL/PVP/100	100	0

The total amount of polymer in the polymer solutions was kept constant at 0.5 g. Accordingly, the drug amounts per g polymer for PCL/PVP/C, PCL/PVP/50, PCL/PVP/75 and PCL/PVP/100 fiber groups were obtained as 0.25, 0.37 and 0.50 mg GSK2126458, respectively.

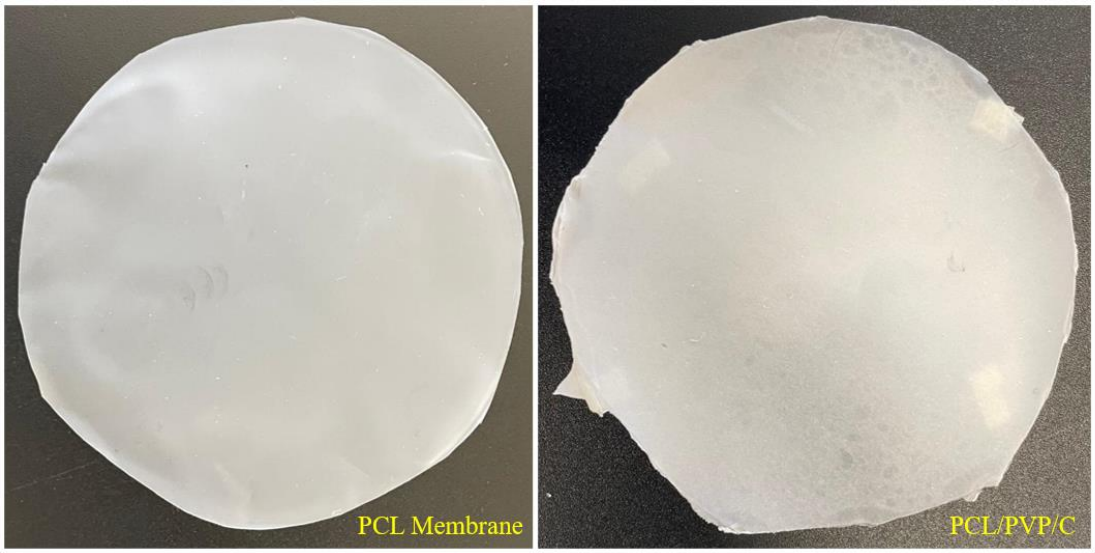

Figure 4.9. Image PCL membrane and fiber production by electrospinning on PLC membrane.

The produced fiber membranes were left to dry at room temperature for 24 hours. At the end of 24 hours, they were stored at -20°C to be used in experiments. Membranes were cut into 1.5 cm diameter for cell culture and antibacterial activity studies.

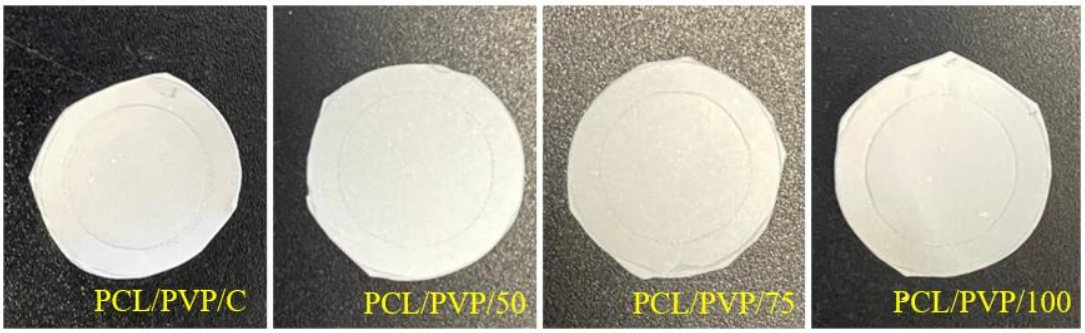

Figure 4.10. Image of fiber membranes produced by electrospinning on PCL membrane with a diameter of 1.5 cm.

4.3. Characterization of Drug Loaded PCL/PVP Fibers

4.3.1. SEM and diameter distribution analysis

SEM analysis results of fiber membrane groups are given in Figure 4.11.

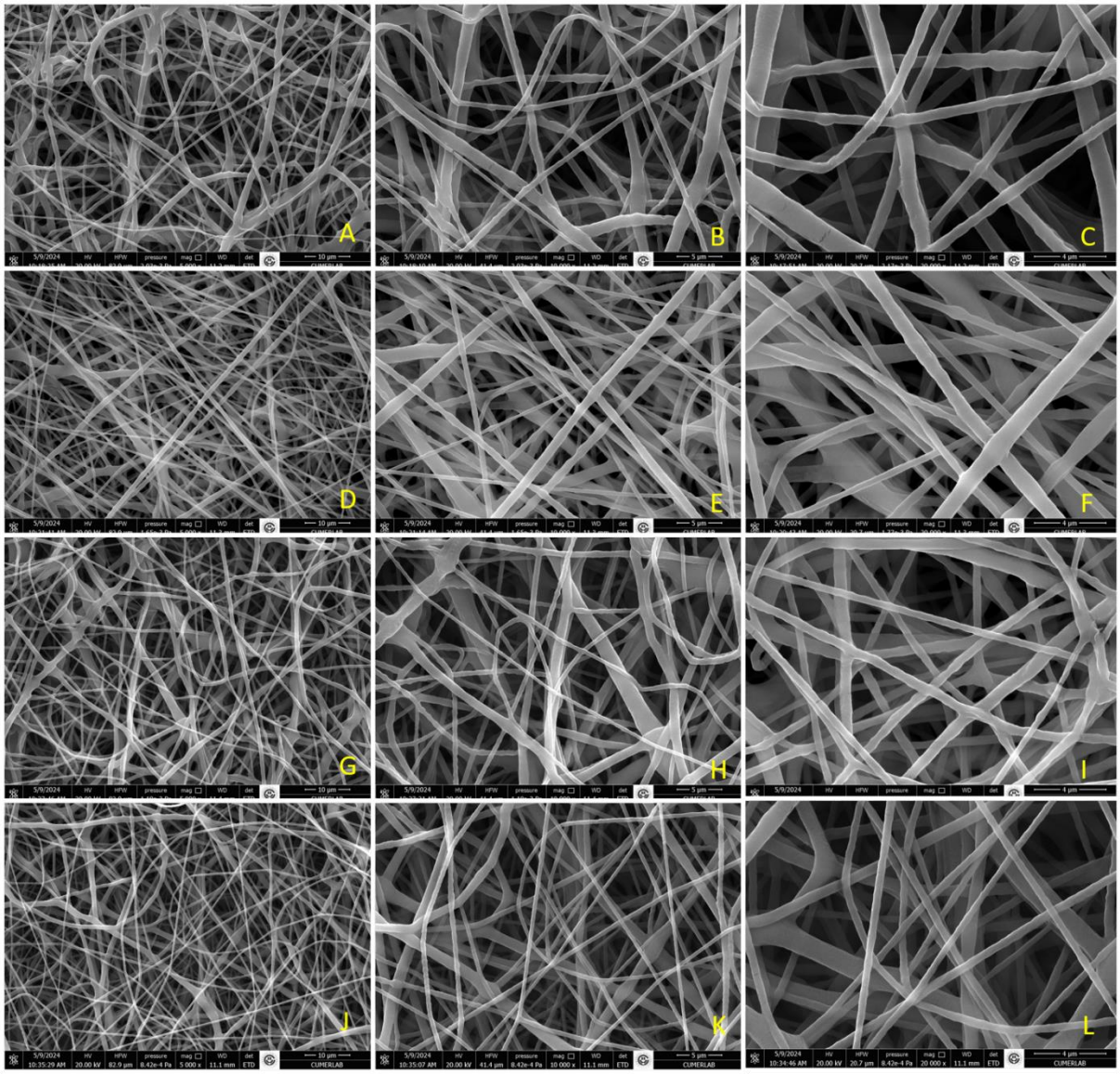

Figure 4.11. Images of PCL/PVP/Control (A-C), PCL/PVP/50 (D-F), PCL/PVP/75 (G-I) and PCL/PVP/100 (J-L) groups obtained by SEM analysis. 5000 magnification (A, D, G, J), 10000 magnification (B, E, H, K), and 20000 magnification (C, E, I, L).

ImageJ software was used to calculate average fiber diameters and fiber diameter distributions using SEM images. Diameter distrubutions of fibers are given in Figure 4.12.

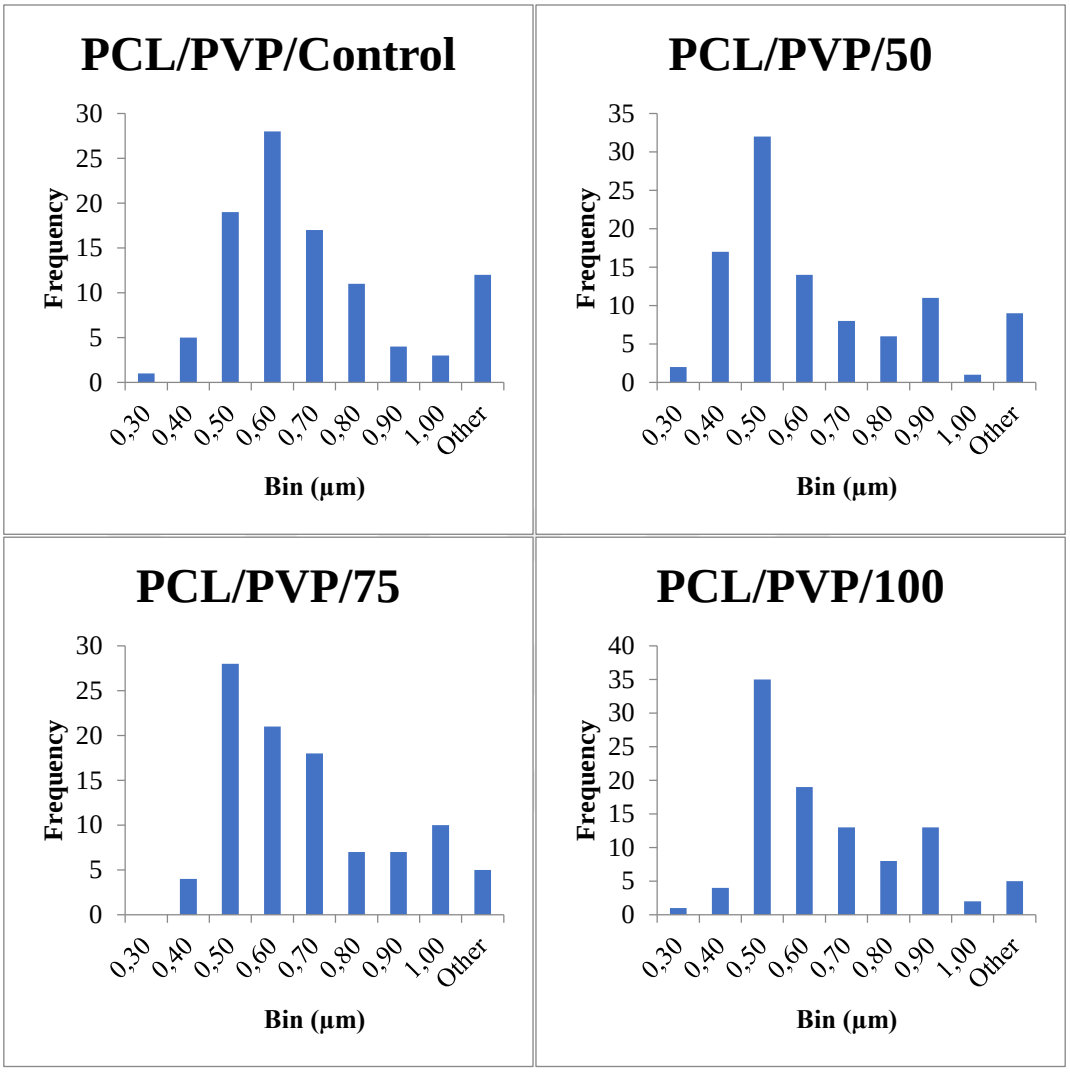

Figure 4.12. Diameter histogram graphs of fibers.

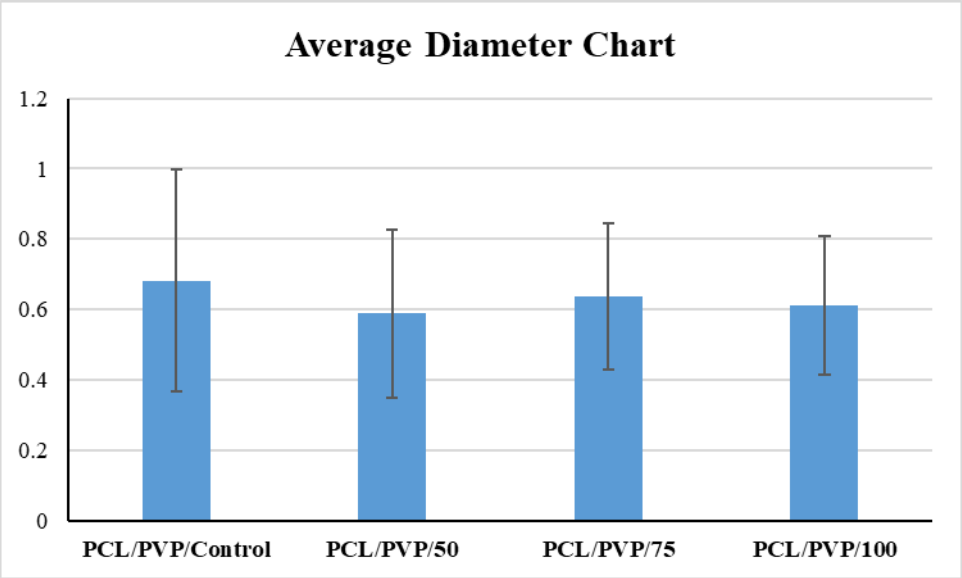

Figure 4.13. Graphical display of average fiber diameters and standard deviations of fibers.

Table 4.3. Average fiber diameters.

Sample	Average fiber diameters (μm)
PCL/PVP/C	0.682 ± 0.316
PCL/PVP/50	0.588 ± 0.240
PCL/PVP/75	0.637 ± 0.208
PCL/PVP/100	0.611 ± 0.196

SEM images indicated that smooth and continuous fiber structures were obtained in all groups. The fibers were also beading free. Average diameters of the fibers were calculated as 0,682 ± 0,316 μm, 0,588 ± 0,240 μm, 0,637 ± 0,208 μm, and 0,611 ± 0,196 μm for PCL/PVP/C, PCL/PVP/50, PCL/PVP/75 and PCL/PVP/100 groups, respectively. Statistical analysis indicated that there were no significant differences in the fiber diameter between groups. This was considered to be a result of the fact that the polymer type, the amount and the amount of solvent in which the GSK2126458 was dissolved were the same for all groups. Therefore, there was no significant difference neither in the structure of the fibers nor in the diameter distribution of the fibers. There were some thin and some thick fibers in all fiber structures. This may due to the use of different polymer types in the fiber structure.

4.3.2. FTIR analysis

FTIR spectra of PCL/PVP fiber membranes collected on aluminum foil with or without GSK2126458 drug molecule are given in Figure 4.14 and Figure 4.15. The fiber samples were removed from aluminum foil before analysis. Main peaks for PCL polymer were recorded at 1165 cm^{-1}, 1240 cm^{-1}, 1722 cm^{-1}, 2866 cm^{-1}, and 2945 cm^{-1} [45], [46]. The peaks at 2866 cm^{-1}, and 2945 cm^{-1} wavelengths were attributed to asymmetric and symmetric vibrations of CH2 group. The peaks recorded at 1240 cm^{-1} and 1165 cm^{-1} wavelengths are asymmetric and symmetric C-O-C stretching, respectively [47]. The peak obtained at 1722 cm^{-1} is seen as the stretching of the C=O ester carbonyl group of the crystalline structure [45].

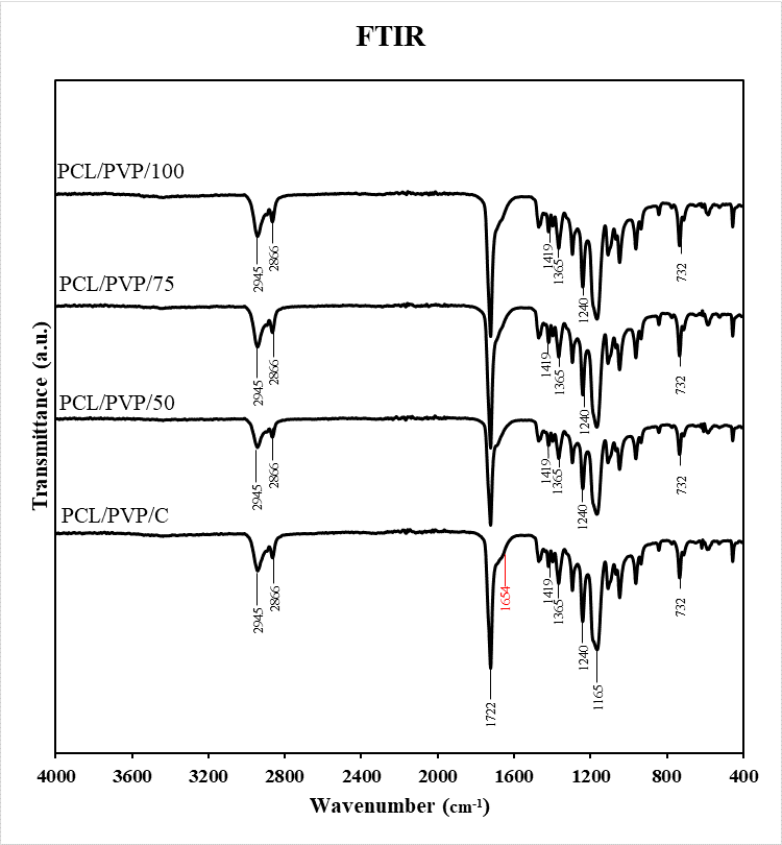

Figure 4.14. FTIR spectra of PCL/PVP fibers.

Main FTIR peaks for PVP polymer were given as a carbonyl stretching band, CH bending and CH2 wagging and CN stretch around 1650 cm−1, 1374 cm−1, and 1277 cm−1, respectively [47] and generally overlapped with PCL peaks. However, there was not any peak in the FTIR spectrum of pure PCL around 1650 cm−1 [45] so, in this study the neck around 1654 cm-1

was attributed to the CN stretch of PVP polymer indicating the presence of low amount of PVP in PCL/PVP blend. As a result, it was concluded that the PCL/PVP fibers produced in this thesis study contained predominantly PCL as desired. In addition, in the study conducted by Massoumi et al. [48], the FTIR results for PCL were found to be consistent with the FTIR results of the PCL/PVP fiber groups produced in this thesis.

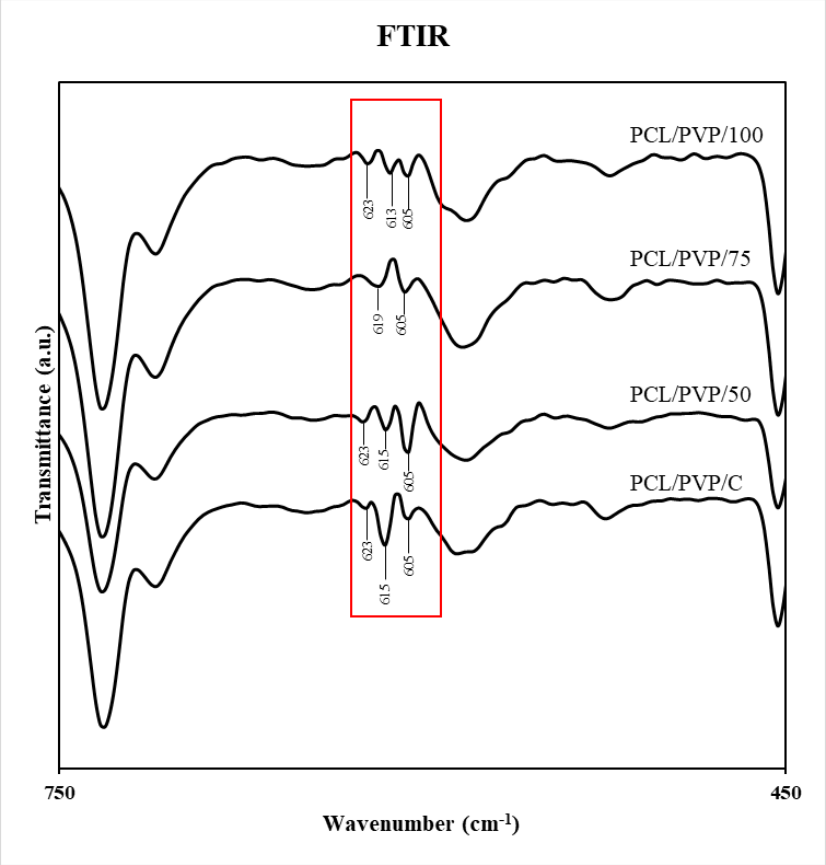

Figure 4.15. Detailed FTIR spectra of PCL/PVP fiber membranes.

There was a little difference between 605 cm^{-1} to 623 cm^{-1} wavelengths for control and drug loaded fiber membranes. The peak at 615 cm^{-1} which corresponds to C-H bending [49] was shrunked with increasing drug concentration as shown in Figure 4.15. This little change was probably due to the very low amount of drug molecule and its encapsulation in the polymer structure.

4.3.3. Contact angle analysis

In this analysis, contact angle measurements were performed to determine the wettability properties of fiber groups containing different amounts of drug. For contact angle analysis, 1x1 cm dimensions were cut from the electrospun samples of PCL/PVP/C, PCL/PVP/50, PCL/PVP/75 and PCL/PVP/100 fiber groups on aluminum foil. Three samples were cut for each group and the analyses were completed in triplicate. The average contact angles were determined according to the results of the contact angle analyses.

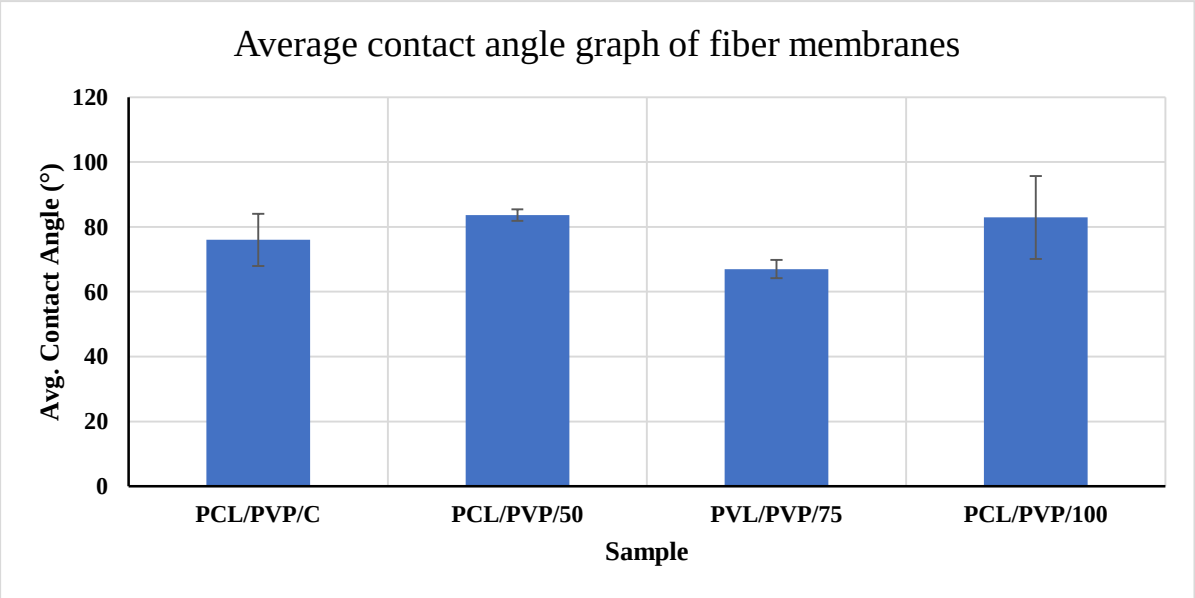

Figure 4.16. Graph of average contact angle of fiber groups.

Table 4.4. Average contact angle (ACA) values.

Sample	ACA (°)
PCL/PVP/C	76.02 ± 8.06
PCL/PVP/50	83.63 ± 1.75
PVL/PVP/75	66.98 ± 2.83
PCL/PVP/100	82.92 ± 12.82

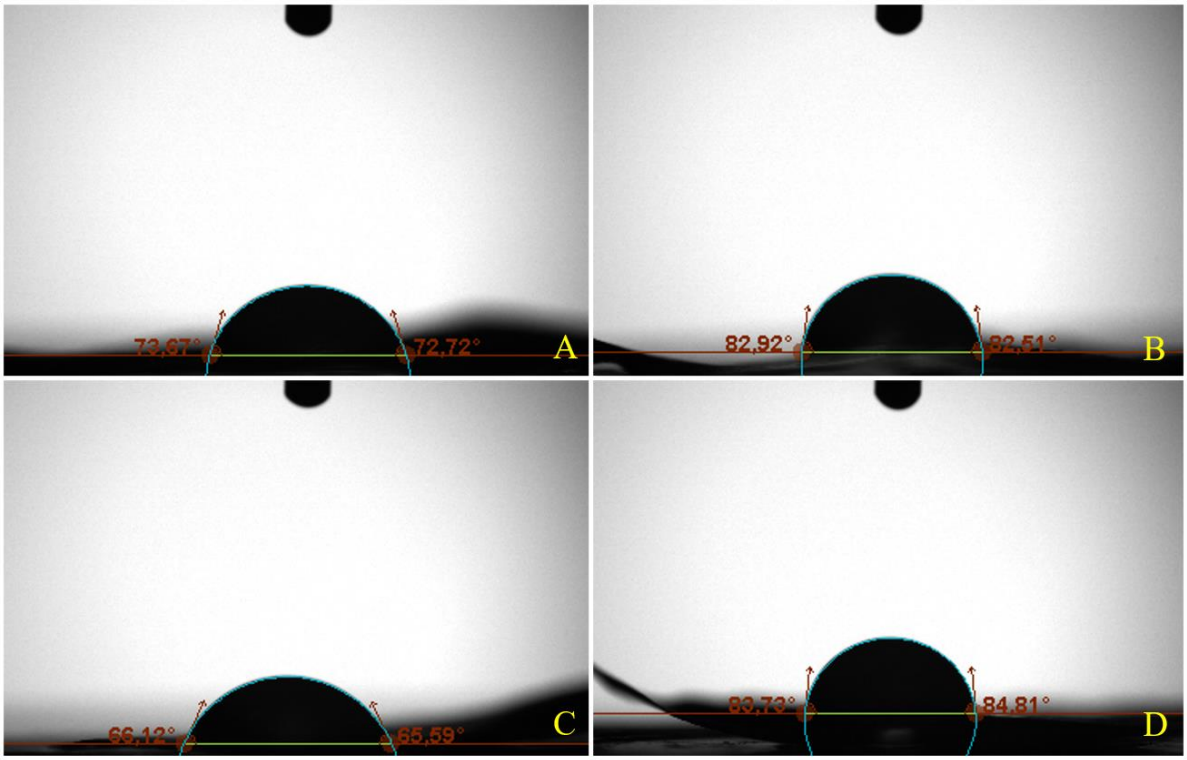

Figure 4.17. Images of contact angle of fiber groups. Images chosen as closest to average contact angle values. PCL/PVP/C (A), PCL/PVP/50 (B), PCL/PVP/75 (C) AND PCL/PVP/100 (D).

The data obtained as a result of contact angle analysis were compared with the studies in the literature. In the study conducted by Marmur et al. [50], on contact angles on different surfaces, the material obtained with a contact angle above 90° is considered hydrophobic. For materials with a contact angle below 90°, the material is considered hydrophilic [50]. According to the contact angle results, it was observed that the materials used in this study had average contact angle values below 90°. Considering these results, it was concluded that the materials were hydrophilic. Contact angles were similar between PCL/PVP fiber groups. It was observed that the wettability properties of the GSK2126458 drug used in this study did not increase the hydrophilic properties of the fibers depending on the drug concentration. In other words, it was concluded that the hydrophilic properties of the fibers did not increase as the drug concentration in the fibers increased.

4.3.4. Texture analysis

One of the mechanical analyses among the characterization analyses of fiber structures is texture analysis. During texture analysis, fiber groups were cut into 1x4 cm dimensions. Fibers cut to the desired dimensions were subjected to tensile-tension tests.

Table 4.5. Table of tensile-tension analysis results of PCL/PVP/C fiber group.

Sample	**Strength MPa**	**Toughness (MJ/m^3)**	**Young Modulus (MPa)**	**Elongation at Break %**
PCL/PVP/C-1	2.20	1.08	15.46	65.71
PCL/PVP/C-2	4.75	2.44	32.82	73.56
PCL/PVP/C-3	3.04	1.53	11.24	74.46
PCL/PVP/C-4	2.99	1.09	26.97	50.27
PCL/PVP/C-5	2.69	0.98	10.16	51.95
PCL/PVP/C-6	3.38	0.89	55.52	35.76
Avg.	3.17	1.34	25.36	58.62
SD	0.87	0.58	17.30	15.24

SD: Standard deviation

Table 4.6. Table of tensile-tension analysis results of PCL/PVP/50 fiber group.

Sample	Strength MPa	Toughness (MJ/m^3)	Young Modulus (MPa)	Elongation at Break %
PCL/PVP/50-1	7.43	3.79	86.22	69.53
PCL/PVP/50-2	0.86	0.06	97.94	8.16
PCL/PVP/50-3	9.16	6.19	92.79	95.44
PCL/PVP/50-4	3.45	0.68	41.54	26.44
PCL/PVP/50-5	8.52	4.60	138.19	71.29
PCL/PVP/50-6	1.65	0.17	90.36	13.47
PCL/PVP/50-7	1.82	0.22	60.24	15.30
Averages	4.70	2.25	86.75	42.80
SD	3.55	2.55	30.46	35.08

SD: Standard deviation

It was determined by both SEM images and FTIR analysis that there was no structural difference between the fiber groups. Therefore, only PCL/PVP/C and PCL/PVP/50 group fibers were tested in the tensile analysis.

4.4. Cell Culture Studies Results

B16-F10, mouse melanoma cell line between passage 44-47 was used in cell culture studies. Cells were cultured on 75 cm^2 TCPS and cell density was calculated as 114.800 cells/cm^2 when they were confluence on the surface.

In Figure 4.18, surface adhesion and spreading of B16-F10 cells are clearly seen in light microscope images. The cells showed fibroblast morphology with their starlike shapes. B16-F10 cells are described as a cell line exhibiting a morphology of spindle-shaped and epithelial-like cells" by American Type Culture Collection (ATCC). In our study most of them showed spindle-shaped or star-like shaped morphology. This might probably because of the passage number of the cells. The cells were at passage 44 in Figure 4.18. DAPI staining was conducted to show both morphology of cell nuclei and if there was any mycoplasma contamination. Nuclei of the cells showed circular morphology in general and some of them showed elongated shape. The same results were demonstrated in the study conducted by Biggers et al. for B16-F10 cells [51]. This may vary according to the stage of cell attachment. More spreading cells may show an elongated nucleus shape. DAPI staining images also showed that the B16-F10 cell line at passage 44 was clear for DAPI staining without suspicion of any mycoplasma contamination.

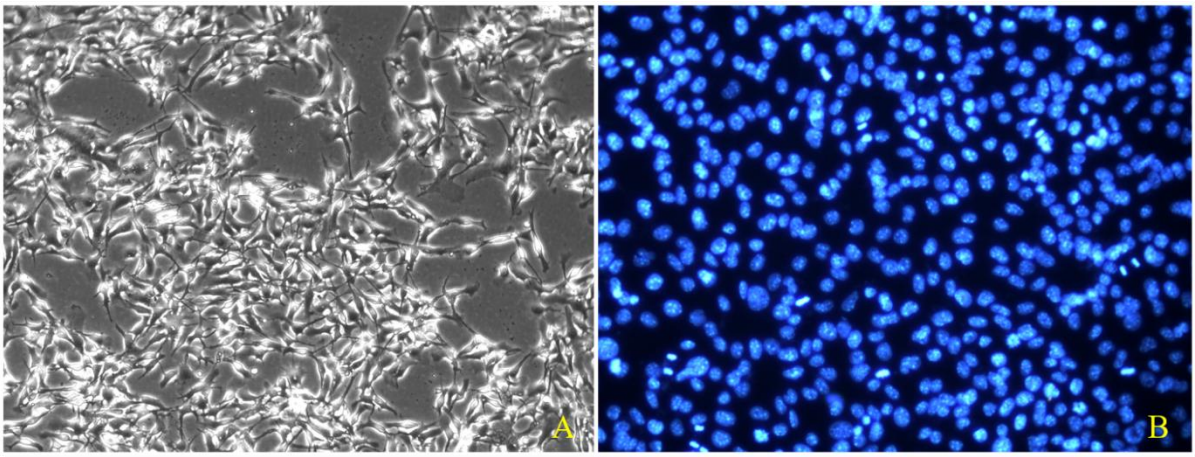

Figure 4.18. Phase contrast image of the B16-F10 cell line used in cell culture studies (10X) and DAPI (blue) images of the cells at passage 44 (20X).

4.4.1. Determination of IC_{50} for GSK2126458

To determine the IC_{50} value of GSK2126458 drug, the cells were cultured on 96 well plate. They were seeded at a concentration of 10,000 cells / well in 200 µL cell culture medium. The cells were incubated at 37^{o}C in 5% CO_2 atmosphere in for 24 hours. At the end of cell incubation, growth media were replaced with growth media containing different drug concentrations, DMSO at 1/1000 dilution as solvent control group and control group without drug and DMSO. Drug concentrations were selected as 50, 40, 30, 20, 10, 5, 2.5, 1.25, 0.625, and 0.315 µM. The cells were incubated another 24 hour at 37 ^{o}C in 5% CO_2 atmosphere. Serum containing complete growth medium was used in the study. Cell viabilities were determined resazurin analysis as described in materials and methods section. Inverted phase contrast images of the cells used in cell viability stuy are given in Figure 4.19.

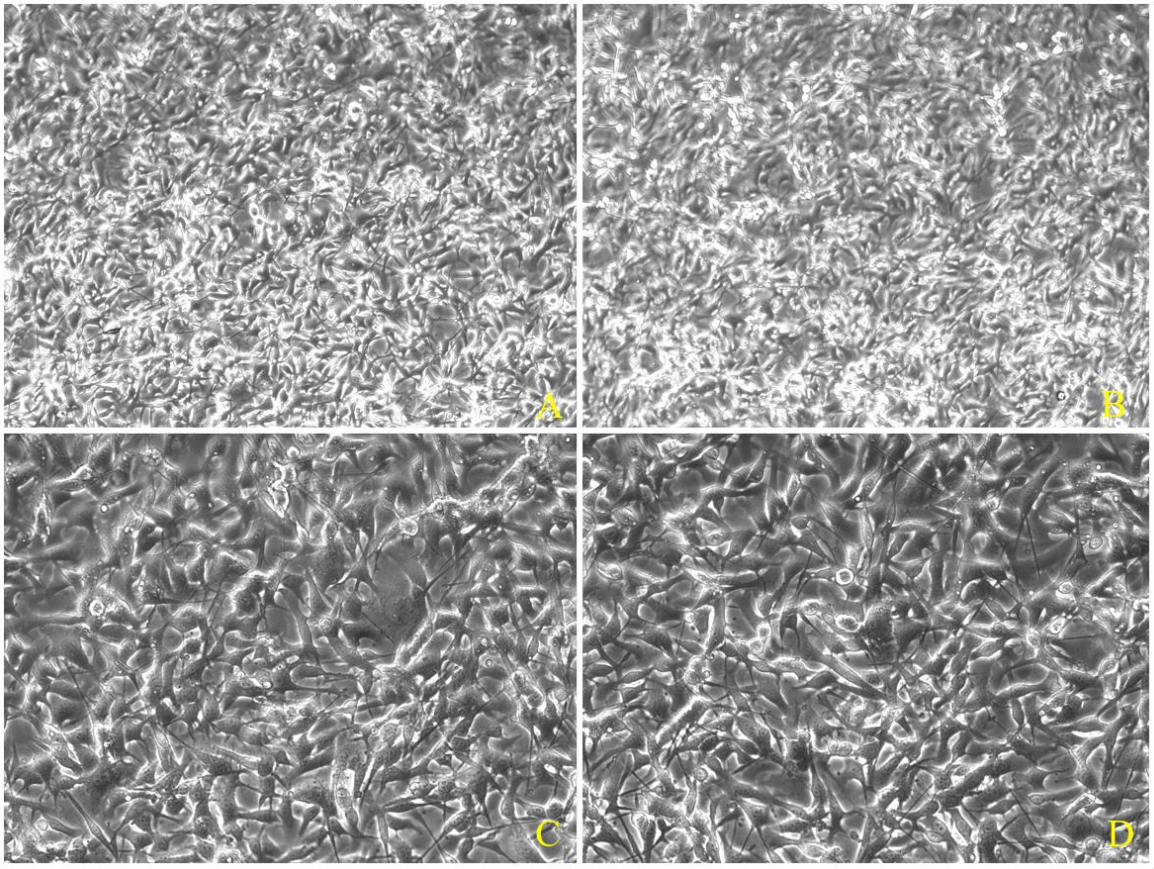

Figure 4.19. 10x (A-B) and 20x (C-D) phase contrast images of the B16-F10 cells in the T75 flask used in cell culture studies.

%Cell viabilities are given in Figure 4.20. IC_{50} concentration of GSK2126458 drug molecule on B16-F10 cell line was calculated using viability results as shown in Figure 4.21.

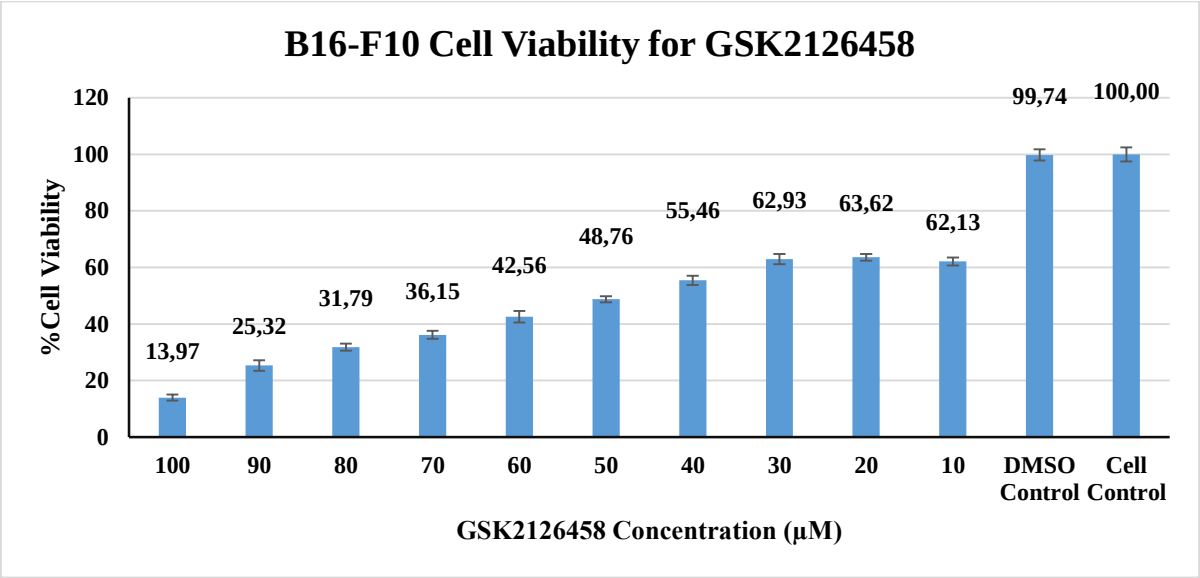

Figure 4.20. %Cell viabilities at different concentrations of GSK2126458 drug as a result of resazurin analysis.

According to viability analysis results, a slope graph was created to obtain the IC_{50} value using 100-90-80-70-60-50-40-30-0 µM concentrations.

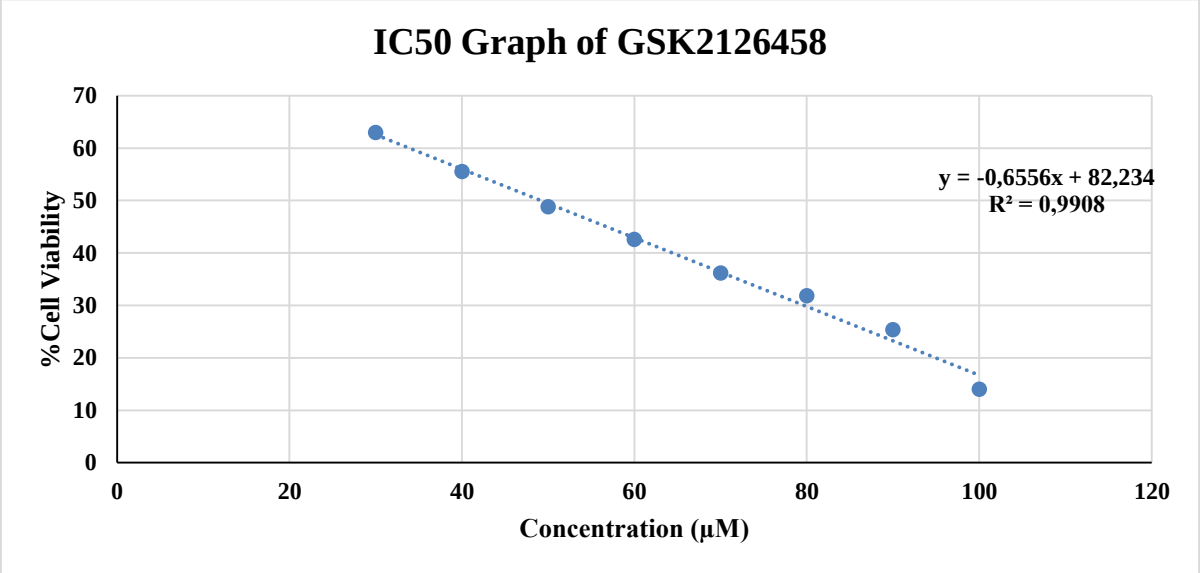

Figure 4.21. Slope graph of the values at which 50% cell viability is obtained from cell viability analysis.

According to the results of the viability analysis, the concentration range in which 50% viability was observed was selected and the slope graph and equation were obtained.

$$y = -0.6556x + 82.324 \qquad \textit{(Equation 1)}$$

According to *Equation 1*, the IC_{50} value was calculated as 49.21 μM GSK2126458.

In a by Khalili et al., the effects of the clinically important PI3K inhibitor GSK2126458 molecule on mutated uveal melanoma cells were investigated. At the end of the study, it was stated that the PI3K inhibitor GSK2126458 drug molecule treatment caused a decrease in cell growth and cell cycle arrest [52]. In the study conducted by Krepler et al., live tissue samples were taken from patients. Resistance mechanisms were defined as against targeted therapy. These mechanisms generally lead to reactivation of the MAPK signaling pathway or activation of the PI3K signaling pathway. Some preclinical data indicated that combinations of BRAF/MEK and PI3K/mTOR inhibitors may be effective in BRAF mutant melanomas. Some of the Phase I clinical studies using this combination have indicated the safety of this approach and some clinically active results [53]. In the study conducted by Guo et al., omipalisib, GSK2126458, a specific inhibitor of the mTOR signaling pathway, was applied to melanoma cells. As a result of the application, omipalisib was reported to inhibit growth in melanoma cells and facilitate apoptosis in combination studies [54]. In the study conducted by Chuoi and colleagues, they tested PI3K inhibitors directly on animals by intralesional injection into the paws and ears. Researchers who used omipalisib for the PI3K inhibitor stated that omipalisib treatment caused hypopigmentation in the dermis region and almost complete destruction of melanocytes [55]. In the study conducted by Abbas et al., they stated that omipalisib drug molecule was used in Phase I clinical studies. In addition, the number of combination studies of omipalisib drug molecule with chemotherapeutic agents has increased [56].

4.4.2. Cell viability analysis on PCL/PVP fiber membranes

B16-F10 %cell viabilities at 24 h / 48 h are given in Figure 4.22. According to 24 h viability analysis, %cell viability of PCL/PVP/50, PCL/PVP/75 and PCL/PVP/100 fiber membranes compared to PCL/PVP/C fiber membrane was obtained as 72.25%, 64.61% and 57.82%, respectively. According to 48 h viability analysis, %cell viability of PCL/PVP/50, PCL/PVP/75 and PCL/PVP/100 fiber membranes compared to PCL/PVP/C fiber membrane was obtained as 74.76%, 70.85% and 60.19%, respectively. The %cell viability value of the

TCPS control group was obtained as 116.32% when the PCL/PVP/C fiber membrane group was taken as control.

It was obtained that as the GSK2126458 drug molecule in PCL/PVP fiber membranes increased, B16-F10 %cell viability decreased. As a result of statistical analysis, it was found that there was a significant difference between PCL/PVP/C and PCL/PVP/100 fiber membranes ($p=0.0414$) in the 24 h viability analysis. In the 48 h viability analysis, it was found that there were significant differences between PCL/PVP/C and PCL/PVP/75 fiber membranes ($p=0.0248$) and between PCL/PVP/C and PCL/PVP/100 fiber membranes ($p=0.0059$). In the literature, there is no study in which GSK2126458 drug molecule was loaded into any polymer structure and applied to cells according to authers knowledge.

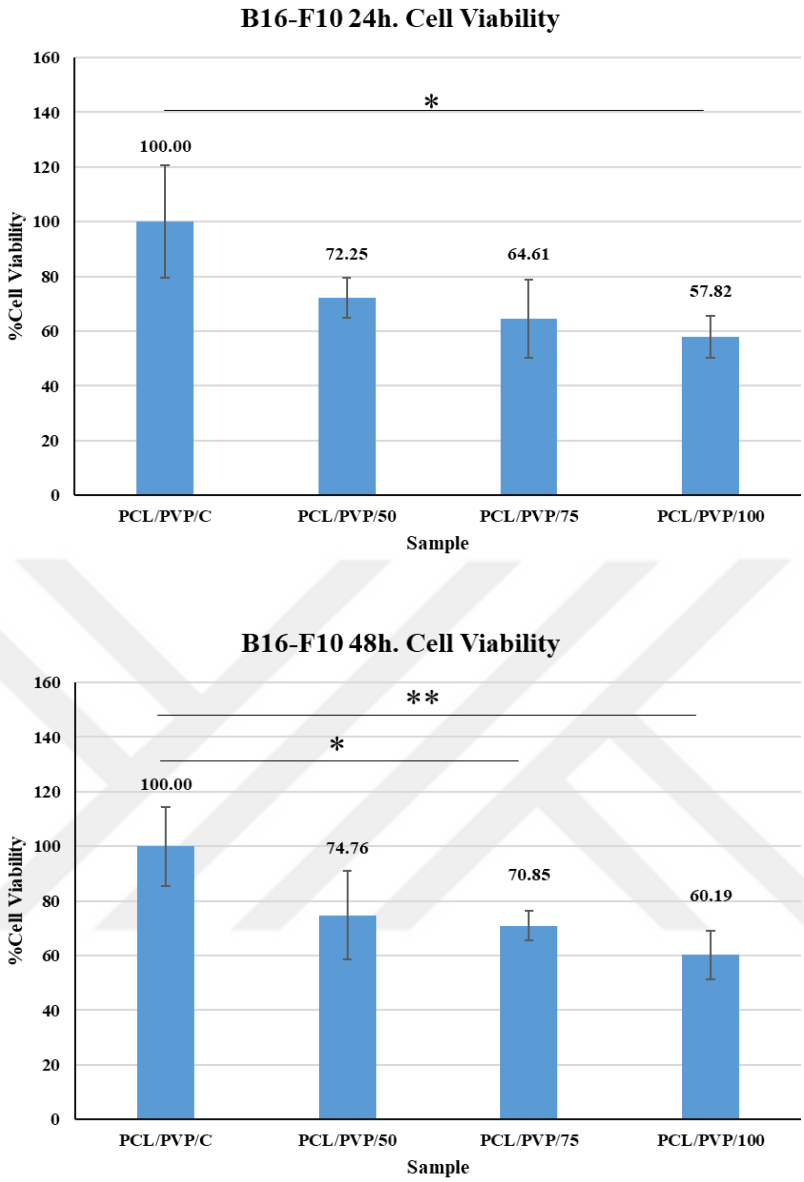

Figure 4.22. Cell viabilities on PCL/PVP fiber membranes at 24 and 48 hour by Resazurin assay.

4.4.3. Visualization of cells on fiber membranes with SEM

SEM images of B16-F10 cells on fiber membranes are given in Figure 4.23. B16-F10 cells spread well on both on control and GSK drug loaded membranes as seen in Figure 4.23. When the morphology of the cells on the membranes with and without drug molecules was compared, it was observed that in the control membranes the cells were spread over a wider area and the boundaries were not very clear, while in the drug-loaded membranes the cell boundaries were clear and the cells were less spread. There were some small crystalline structures on the cells cultured on PCL/PVP/75 fiber membranes. They were probably due to the salt residues after washing with PBS.

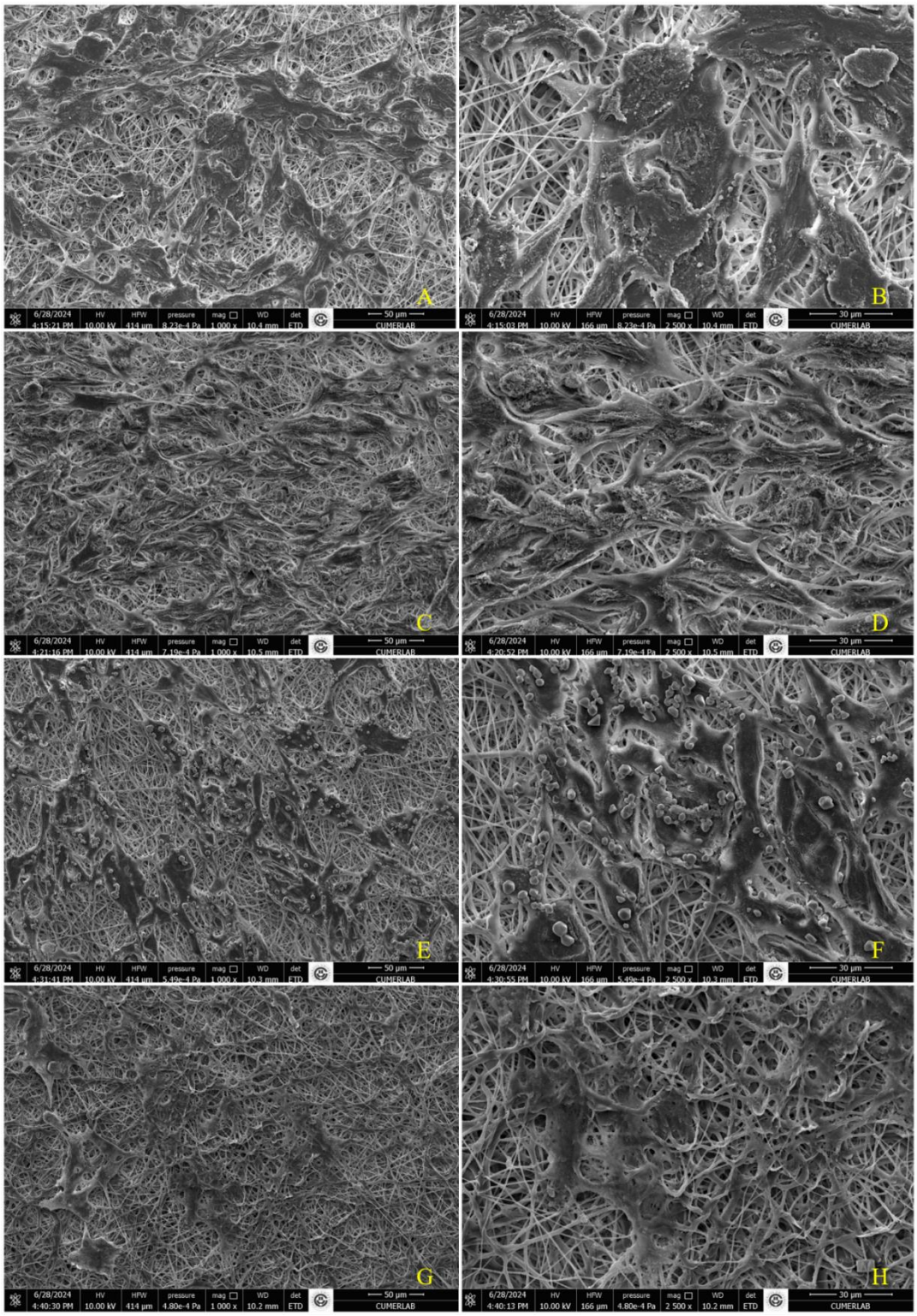

Figure 4.23. SEM images of 24h. viability analysis of PCL/PVP/Control (A-B), PCL/PVP/50 (C-D), PCL/PVP/75 (E-F) and PCL/PVP/100 (G-H) groups obtained as a result of SEM analysis. 1000X magnification (A, C, E, G) and 2500X magnification (B, D, F, H).

4.4.4. Immunofluorescent staining

Immunofluorescence staining was conducted to show both cytoskeletal (F-actin) and nuclear (DAPI) changes of B16-F10 cells cultured on GSK2126458 loaded PCL/PVP membranes. DAPI staining images are given at 4x magnification to show the cell density and cell seeding boundiries in Figure 4.24. DAPI staining showed that cell nuclear morphology was not disrupted with increasing drug concentration, but the live cell density decreased with increasing drug concentration. In cell culture studies the cells were seeded in small volume as a dot shape. DAPI staining does not directly show the cell density on PCL/PVP membanes however it can be used to predict/show cell migration according to the staining area and intensity. The extracellular spaces between the cells and the border where cell seeding takes place are more clear when compared to the other groups which may be an indication of low cell migration from the seeded area.

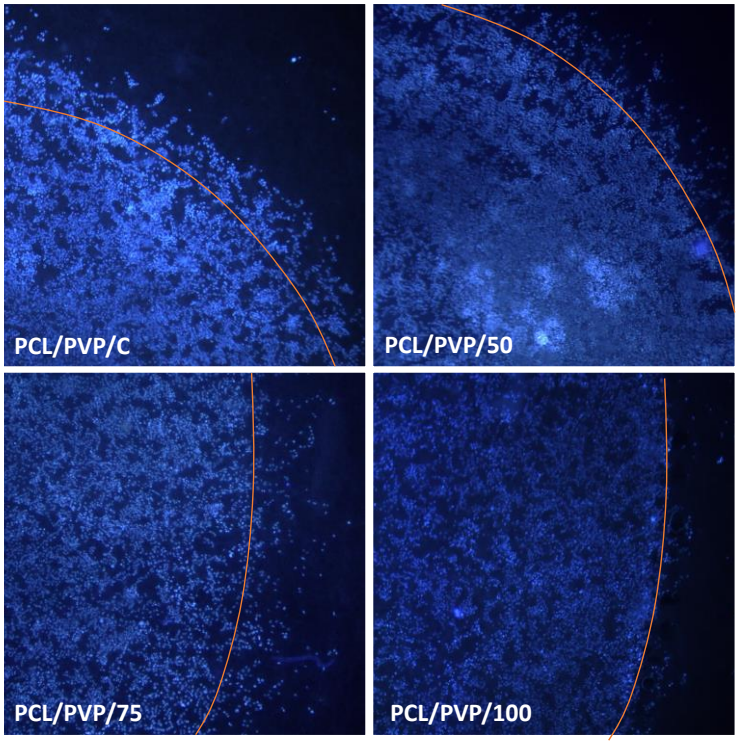

Figure 4.24. Fluorescence microscope images of DAPI (blue) staining of B16-F10 cells on PCL/PVP fiber membranes. Images were obtained at 4x magnification. Orange lines indicate the estimated seeding boundaries of the cells.

DAPI and F-actin staining images of the cells cultured on PCL/PVP membranes are given in Figure 4.25. Decrease in cell density on the membarenes with increasing drug concentration was clearly seen in the image. There was not any significant difference in F-actin staining intensity of the cells on different fiber membranes.

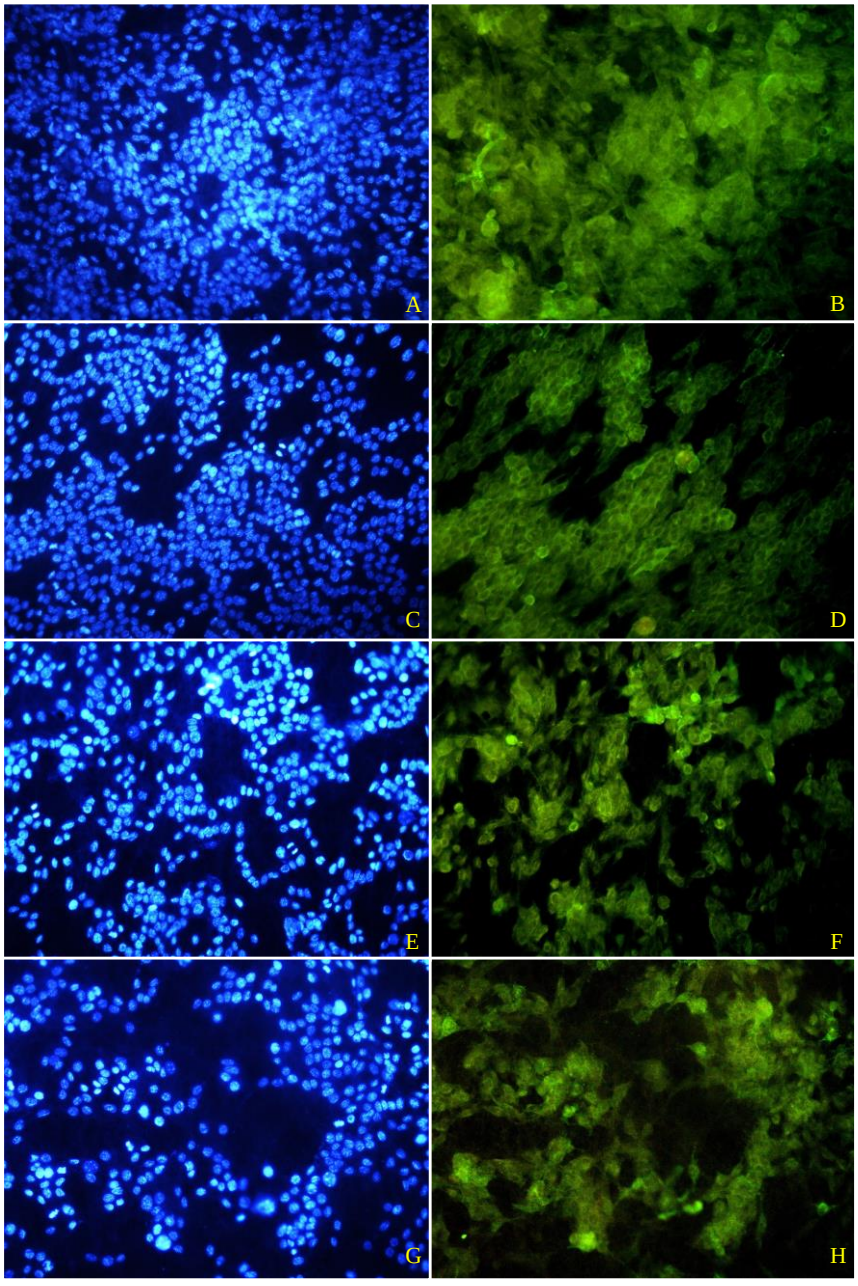

Figure 4.25. Fluorescence microscope images of DAPI (blue) and F-Actin (green) staining of B16-F10 cells on PCL/PVP fiber membranes. Images were obtained at 20x magnification. PCL/PVP/C (A-B), PCL/PVP/50 (C-D), PCL/PVP/75 (E-F) AND PCL/PVP/100 (G-H).

4.5. Antibacterial Analyzes Results

4.5.1. Antibacterial activity determination of PCL/PVP fiber membranes

To measure the antibacterial activities of fiber membranes, 0.5 McFarland bacterial concentration of *E. coli*, *S. aureus*, *P. aeruginosa* and *Methicillin-resistant Staphylococcus aureus* (*MRSA*) bacteria were prepared in PBS. 100 µL of 0.5 McFarland bacteria were inoculated into petri dishes containing nutrient agar (NA) using the spreading method. After bacterial inoculation, 1.5 cm diameter fiber membranes were placed on each side sterilized with UV light for 1.5 hours. Incubation period was waited for 24 hours at 37°C. At the end of 24 hours, it was observed that no inhibition zone was formed around the fiber membranes.

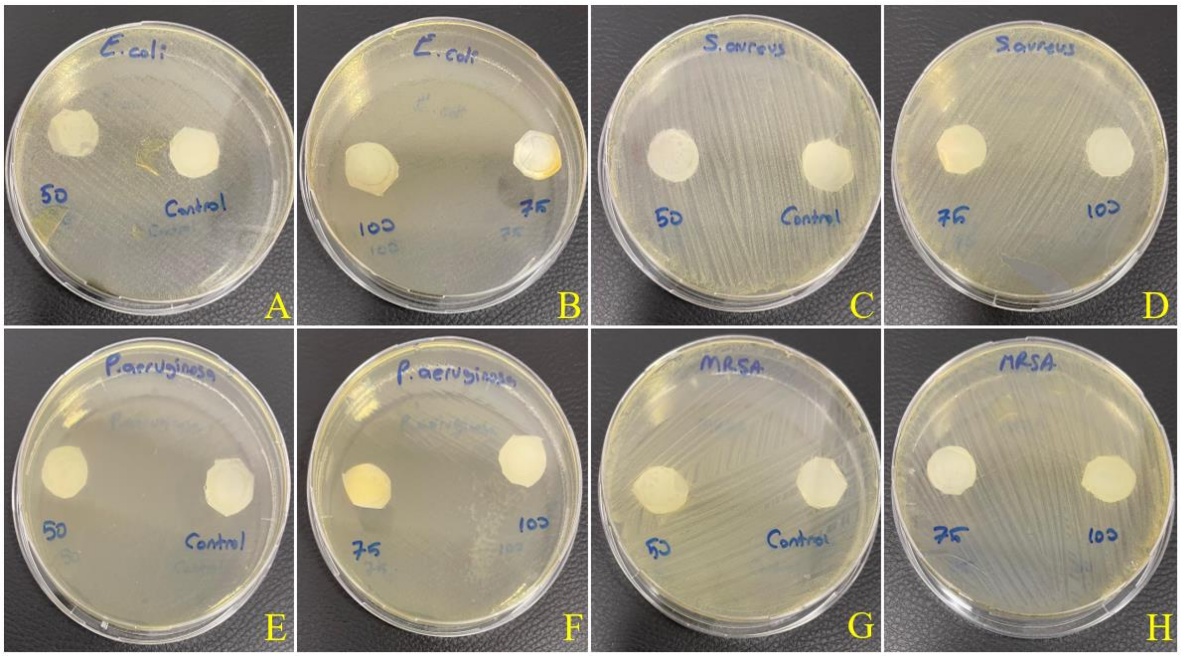

Figure 4.26. Images of fiber membranes after 24 hours of incubation. *E. coli* (A-B), *S. aureus* (C-D), *P. aeruginosa* (E-F) and *MRSA* (G-H)

4.5.2. Disc diffusion assay

The analysis of whether GSK2126458 drug used in fiber production has antibacterial effect was done by disc diffusion analysis. 0.5 McFarland bacterial concentration of *E. coli*, *S. aureus*, *P. aeruginosa* and *Methicillin-resistant Staphylococcus aureus* (*MRSA*) bacteria were prepared in PBS previously. 100 µL of bacterial concentrations were taken and inoculated on petri dishes containing nutrient agar (NA) using the spreading method. At the end of bacterial inoculation, 2 empty and 1 antibiotic containing disks were placed in the petri dishes. 15 µL, 1 mM GSK2126458 dissolved in DMSO previously was dropped on one of the empty disks and 15 µL sterile DMSO was dropped on the other empty disk. Incubation period was waited for 24 hours at 37°C. At the end of 24 hours, no inhibition zone was observed around the drug and DMSO disks except for the antibiotic disks.

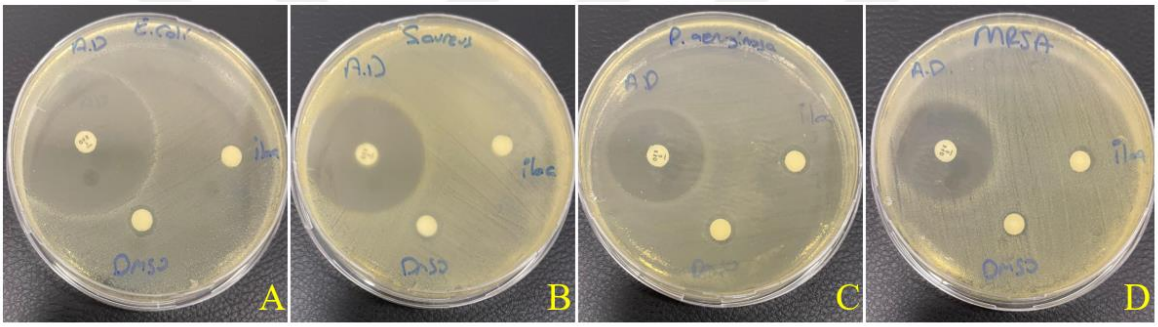

Figure 4.27. Images of inhibition zones of antibiotic, GSK2126458 and DMSO discs. *E. coli* (A), *S. aureus* (B), *P. aeruginosa* (C) and *MRSA* (D).

5. CONCLUSIONS

In this thesis study, GSK2126458 drug molecule which is a highly selective inhibitor for PI3K was loaded in PCL/PVP fiber membranes at different concentrations and their use as an alternative or adjunctive treatment method in melanoma treatment was determined as the main target.

According to the results obtained within the scope of this thesis study:

PCL (Avg. MW: 80,000), PVP (Avg. MW: 10,000), and PVP (M_r: 1,100,000.00) polymer were used to obtain smooth and flat PCL/PVP fibers by electrospinning method. Different electrospin conditions with varying polymer type and concentration, solvent type and concentration, distance, voltage and collector type were applied and the most appropriate conditions allowing smooth and flat PCL/PVP fibers were selected. It was determined that the condition where 11.5% PCL and 0.5% PVP polymers were dissolved in DCM:DMF (1:1) so that the total polymer amount would be 12% and 0.04 mL/min flow rate, 15 cm distance and 24 kV voltage conditions were suitable for the production of smooth and flat fibers.

PCL/PVP fiber membranes with 0, 50, 75 and 100 µL of 10 mM GSK2126458 drug were produced and stored at -20 degrees for cell culture, microbiology and for characterization studies.

The morphology of the fiber membranes were determined by SEM analysis and the average diameters of these fibers were calculated from the SEM images using Image J program. Smooth fibers without any beeding were obtained applying selected elecrospinning conditions. The average diameters for the PCL/PVP/C, PCL/PVP/50, PCL/PVP/75 and PCL/PVP/100 fiber groups were 0.682 ± 0.316, 0.588 ± 0.240, 0.637 ± 0.208 and 0.611 ± 0.196 µm, respectively. Changing amount of GSK2126458 drug neither affected fiber diameter nor fiber morphology significantly.

FTIR spectra of fiber membranes indicated mean peaks for PCL and PVP polymers and specific peaks for PVP polymer overlapped with PCL polymer due to low amount of PVP in polymer blend. FTIR peaks for GSK2126458 drug was not clearly shown in PCL/PVP fiber

membranes. This was probably due to the very low amount of drug molecule and its encapsulation in the polymer structure.

The hydrophilic properties of the fiber groups were analyzed by water contact angle. The average water contact angles for the PCL/PVP/C, PCL/PVP/50, PCL/PVP/75 and PCL/PVP/100 fiber groups were 76.02 ± 8.06, 83.63 ± 1.75, 66.98 ± 2.83 and 82.92 ± 12.82 degrees, respectively. There was not any significant difference between the contact angles of fiber membranes.

The effects of GSK2126458 molecule and fiber groups on B16-F10 cell line were completed by resazurin viability analysis. IC_{50} value of GSK2126458 drug on B16-F10 mouse melanoma cells were calculated as 49.21 μM. Viabilities of B16-F10 cells on PCL/PVL fiber membranes with or without GSK2126458 drug molecule was also investigated by resazurin analysis at 24 and 48 h. PCL/PVP/C fiber group was used as the control group. Resazurin analysis results were converted to %cell viabilities and they were calculated as 72.25%, 64.61% and 57.82% at 24h, and 74.76%, 70.85% and 60.19% at 48 h for PCL/PVP/50, PCL/PVP/75 and PCL/PVP/100 fiber membranes, respectively.

The adhesion of B16-F10 cells to fiber membranes was confirmed by SEM images. In addition, the images obtained with immunofluorescence staining performed on the fiber groups, showing that the cell density decreased proportional to the increasing amount of GSK2126458 drug molecule in fiber membranes supporting the resazurin viability analysis. There was not any significant change in the nucleus shape of the cells according to DAPI staining images.

Antibacterial analysis of both GSK2126458 drug molecule by disk diffusion analysis and PCL/PVP fiber membranes by direct contact test with and without drug molecule indicated that no inhibition zone occurred after 24 h. GSK2126458 drug molecule did not show any antibacterial effect.

6. RECOMMENDATIONS

Drug release studies from fiber membranes have been attempted, but analysis of the drug molecule GSK2126458 cannot be determined by UV-Vis spectroscopy due to the low amount of drug in the fiber membranes. HPLC or ICP-MS analysis can be performed to show the drug molecule released at different time intervals.

The apoptotic effects of the produced fiber membranes can be planned to be performed with Annexin-V and PI staining. Studies can be carried out to prove the activation of PI3K-AKT-mTOR signaling pathways in cells with the drug molecule.

The effects GSK2126458 loaded fiber membarens can be investigated on non-melanoma cell lines compared to the melanoma cell line used in this study. Behaviour of human melanoma and normal cell lines can also be studied with GSK2126458 loaded fiber membranes.

REFERENCES

[1] L. B. Naves, C. Dhand, J. R. Venugopal, L. Rajamani, S. Ramakrishna, and L. Almeida, "Nanotechnology for the treatment of melanoma skin cancer," *Prog. Biomater.*, vol. 6, no. 1–2, pp. 13–26, 2017, doi: 10.1007/s40204-017-0064-z.

[2] I. Risueño, L. Valencia, J. L. Jorcano, and D. Velasco, "Skin-on-a-chip models: General overview and future perspectives," *APL Bioeng.*, vol. 5, no. 3, pp. 1–12, 2021, doi: 10.1063/5.0046376.

[3] M. Dildar *et al.*, "Skin cancer detection: A review using deep learning techniques," *Int. J. Environ. Res. Public Health*, vol. 18, no. 10, 2021, doi: 10.3390/ijerph18105479.

[4] J. Chandra *et al.*, "Nanotechnology-empowered strategies in treatment of skin cancer," *Environ. Res.*, vol. 235, no. July, p. 116649, 2023, doi: 10.1016/j.envres.2023.116649.

[5] J. Jaworek-Korjakowska and P. Kleczek, "ESkin: Study on the smartphone application for early detection of malignant melanoma," *Wirel. Commun. Mob. Comput.*, vol. 2018, 2018, doi: 10.1155/2018/5767360.

[6] G. V Long, S. M. Swetter, A. M. Menzies, J. E. Gershenwald, and R. A. Scolyer, "Cutaneous melanoma," *Lancet*, vol. 402, no. 10400, pp. 485–502, 2023.

[7] E. Craythorne and F. Al-Niami, "Skin cancer," *Medicine (Baltimore).*, vol. 45, no. 7, pp. 431–434, 2017.

[8] A. J. Miller and M. C. Mihm Jr, "Melanoma," *N. Engl. J. Med.*, vol. 355, no. 1, pp. 51–65, 2006.

[9] B. Domingues, J. M. Lopes, P. Soares, and H. Pópulo, "Melanoma treatment in review," *ImmunoTargets Ther.*, vol. 7, p. 35, 2018.

[10] J. Oba and S. E. Woodman, "The genetic and epigenetic basis of distinct melanoma types," *J. Dermatol.*, vol. 48, no. 7, pp. 925–939, 2021, doi: 10.1111/1346-8138.15957.

[11] M. Ciążyńska *et al.*, "The incidence and clinical analysis of non-melanoma skin cancer," *Sci. Rep.*, vol. 11, no. 1, pp. 1–10, 2021, doi: 10.1038/s41598-021-83502-8.

[12] H. Zeng, J. Li, K. Hou, Y. Wu, H. Chen, and Z. Ning, "Melanoma and Nanotechnology-Based Treatment," *Front. Oncol.*, vol. 12, no. March, pp. 1–6, 2022, doi: 10.3389/fonc.2022.858185.

[13] A. Eftekhari *et al.*, "Current analytical approaches in diagnosis of melanoma," *TrAC Trends Anal. Chem.*, vol. 116, pp. 122–135, 2019.

[14] L. M. Sánchez-Reyes, J. Rodríguez-Reséndiz, S. Salazar-Colores, G. N. Avecilla-Ramírez, and G. I. Pérez-Soto, "A high-accuracy mathematical morphology and multilayer perceptron-based approach for melanoma detection," *Appl. Sci.*, vol. 10, no. 3, 2020, doi: 10.3390/app10031098.

[15] H. Xue, J. Li, H. Xie, and Y. Wang, "Review of drug repositioning approaches and resources," *Int. J. Biol. Sci.*, vol. 14, no. 10, pp. 1232–1244, 2018, doi: 10.7150/ijbs.24612.

[16] J. P. Jourdan, R. Bureau, C. Rochais, and P. Dallemagne, "Drug repositioning: a brief overview," *J. Pharm. Pharmacol.*, vol. 72, no. 9, pp. 1145–1151, 2020, doi: 10.1111/jphp.13273.

[17] S. D. Knight *et al.*, "Discovery of GSK2126458, a highly potent inhibitor of PI3K and the mammalian target of rapamycin," *ACS Med. Chem. Lett.*, vol. 1, no. 1, pp. 39–43, 2010, doi: 10.1021/ml900028r.

[18] "Merck." https://www.sigmaaldrich.com/TR/en/product/sigma/sml3161.

[19] R. Cassano, M. Cuconato, G. Calviello, S. Serini, and S. Trombino, “Recent advances in nanotechnology for the treatment of melanoma,” *Molecules*, vol. 26, no. 4, p. 785, 2021.
[20] H. Mishra, P. K. Mishra, A. Ekielski, M. Jaggi, Z. Iqbal, and S. Talegaonkar, “Melanoma treatment: from conventional to nanotechnology,” *J. Cancer Res. Clin. Oncol.*, vol. 144, no. 12, pp. 2283–2302, 2018, doi: 10.1007/s00432-018-2726-1.
[21] N. Aminu *et al.*, “Applications of nanofibers drug delivery system in cancer therapy,” *J. Drug Deliv. Sci. Technol.*, p. 105128, 2023.
[22] G. Viscusi, G. Paolella, E. Lamberti, I. Caputo, and G. Gorrasi, “Quercetin-Loaded Polycaprolactone-Polyvinylpyrrolidone Electrospun Membranes for Health Application: Design, Characterization, Modeling and Cytotoxicity Studies,” *Membranes (Basel).*, vol. 13, no. 2, 2023, doi: 10.3390/membranes13020242.
[23] L. Castillo-Henríquez, R. Vargas-Zúñiga, J. Pacheco-Molina, and J. Vega-Baudrit, “Electrospun nanofibers: A nanotechnological approach for drug delivery and dissolution optimization in poorly water-soluble drugs,” *ADMET DMPK*, vol. 8, no. 4, pp. 325–353, 2020, doi: 10.5599/admet.844.
[24] L. F. Zhu, Y. Zheng, J. Fan, Y. Yao, Z. Ahmad, and M. W. Chang, “A novel core-shell nanofiber drug delivery system intended for the synergistic treatment of melanoma,” *Eur. J. Pharm. Sci.*, vol. 137, no. July, p. 105002, 2019, doi: 10.1016/j.ejps.2019.105002.
[25] K. Sadeqzadeh *et al.*, “Electrospun nanofibers combined with Fe-doped mesoporous bioactive glass nanoparticles induce in vitro melanoma cell death,” *Ceram. Int.*, 2024.
[26] L. Muthulakshmi *et al.*, “Sodium alginate nanofibers loaded Terminalia catappa scaffold regulates intrinsic apoptosis signaling in skin melanoma cancer,” *Process Biochem.*, vol. 118, pp. 92–102, 2022.
[27] F. Serio *et al.*, “Electrospun polyvinyl-alcohol/gum arabic nanofibers: Biomimetic platform for in vitro cell growth and cancer nanomedicine delivery,” *Int. J. Biol. Macromol.*, vol. 188, pp. 764–773, 2021.
[28] R. Garrett, E. Niiyama, Y. Kotsuchibashi, K. Uto, and M. Ebara, “Biodegradable nanofiber for delivery of immunomodulating agent in the treatment of basal cell carcinoma,” *Fibers*, vol. 3, no. 4, pp. 478–490, 2015, doi: 10.3390/fib3040478.
[29] M. Wang, M. Gao, K. D. Miller, G. W. Sledge, and Q.-H. Zheng, “[11C] GSK2126458 and [18F] GSK2126458, the first radiosynthesis of new potential PET agents for imaging of PI3K and mTOR in cancers,” *Bioorg. Med. Chem. Lett.*, vol. 22, no. 4, pp. 1569–1574, 2012.
[30] L. N. Kwong and M. A. Davies, “Navigating the therapeutic complexity of PI3K pathway inhibition in melanoma,” *Clin. cancer Res.*, vol. 19, no. 19, pp. 5310–5319, 2013.
[31] X. Shi, J. Wang, Y. Lei, C. Cong, D. Tan, and X. Zhou, “Research progress on the PI3K/AKT signaling pathway in gynecological cancer (Review),” *Mol. Med. Rep.*, vol. 19, no. 6, pp. 4529–4535, 2019, doi: 10.3892/mmr.2019.10121.
[32] D. Mondal, M. Griffith, and S. S. Venkatraman, “Polycaprolactone-based biomaterials for tissue engineering and drug delivery: Current scenario and challenges,” *Int. J. Polym. Mater. Polym. Biomater.*, vol. 65, no. 5, pp. 255–265, 2016, doi: 10.1080/00914037.2015.1103241.
[33] S. Suganya, T. Senthil Ram, B. S. Lakshmi, and V. R. Giridev, “Herbal drug incorporated antibacterial nanofibrous mat fabricated by electrospinning: an excellent

matrix for wound dressings," *J. Appl. Polym. Sci.*, vol. 121, no. 5, pp. 2893–2899, 2011.
[34] Y. J. Lee, A. Elosegui-Artola, K. H. T. Le, and G.-M. Kim, "Morphological cues for regulation of cell adhesion and motility with tailored electrospun scaffolds of PCL and PCL/PVP blends," *Cell. Mol. Bioeng.*, vol. 6, no. 4, pp. 482–495, 2013.
[35] M. Afrashi, M. Nasari, D. Semnani, P. Dehghan, and M. Maheronnaghsh, "Comparison of the antifungal activity of fluconazole-and ketoconazole-loaded PCL/PVP nanofibrous mat," *Bull. Mater. Sci.*, vol. 44, no. 2, pp. 1–9, 2021.
[36] L.-F. Zhu, Y. Zheng, J. Fan, Y. Yao, Z. Ahmad, and M.-W. Chang, "A novel core-shell nanofiber drug delivery system intended for the synergistic treatment of melanoma," *Eur. J. Pharm. Sci.*, vol. 137, p. 105002, 2019.
[37] M. Nasari, D. Semnani, M. Hadjianfar, and S. Amanpour, "Poly (ε-caprolactone)/poly (N-vinyl-2-pyrrolidone) core–shell nanofibers loaded by multi-walled carbon nanotubes and 5-fluorouracil: an anticancer drug delivery system," *J. Mater. Sci.*, vol. 55, no. 23, pp. 10185–10201, 2020, doi: 10.1007/s10853-020-04784-3.
[38] T. Liu *et al.*, "Dual PI3K/mTOR inhibitors, GSK2126458 and PKI-587, suppress tumor progression and increase radiosensitivity in nasopharyngeal carcinoma," *Mol. Cancer Ther.*, vol. 14, no. 2, pp. 429–439, 2015, doi: 10.1158/1535-7163.MCT-14-0548.
[39] A. Albawardi, M. Al Ayyan, M. Al Bashir, A. K. Souid, and S. Almarzooqi, "In vitro assessment of antitumor activities of the PI3K/mTOR inhibitor GSK2126458," *Cancer Cell Int.*, vol. 14, no. 1, pp. 1–11, 2014, doi: 10.1186/s12935-014-0090-z.
[40] K. Narov, J. Yang, P. Samsel, A. Jones, J. R. Sampson, and M. H. Shen, "The dual PI3K/mTOR inhibitor GSK2126458 is effective for treating solid renal tumours in Tsc2+/- mice through suppression of cell proliferation and induction of apoptosis," *Oncotarget*, vol. 8, no. 35, pp. 58504–58512, 2017, doi: 10.18632/oncotarget.17215.
[41] H. Park *et al.*, "Synergistic anticancer efficacy of MEK inhibition and dual PI3K/mTOR inhibition in castration-resistant prostate cancer," *Prostate*, vol. 75, no. 15, pp. 1747–1759, 2015, doi: 10.1002/pros.23057.
[42] D. Basu *et al.*, "The dual PI3K/mToR inhibitor omipalisib/GSK2126458 inhibits clonogenic growth in oncogenically-transformed cells from neurocutaneous melanocytosis," *Cancer Genomics and Proteomics*, vol. 15, no. 4, pp. 239–248, 2018, doi: 10.21873/cgp.20082.
[43] Y. Guan, L. Qian, H. Xiao, and A. Zheng, "Preparation of novel antimicrobial-modified starch and its adsorption on cellulose fibers: Part I. Optimization of synthetic conditions and antimicrobial activities," *Cellulose*, vol. 15, no. 4, pp. 609–618, Aug. 2008, doi: 10.1007/s10570-008-9208-6.
[44] Y. Zhang *et al.*, "Bilayer membrane composed of mineralized collagen and chitosan cast film coated with berberine-loaded PCL/PVP electrospun nanofiber promotes bone regeneration," *Front. Bioeng. Biotechnol.*, vol. 9, 2021.
[45] Z. Iyigundogdu, B. S. Petek, M. Capkin Yurtsever, and S. Ceylan, "Melissa officinalis essential oil loaded polycaprolactone membranes: evaluation of antimicrobial activities and cytocompatibility for tissue engineering applications," *Biomed. Mater.*, vol. 18, no. 6, 2023, doi: 10.1088/1748-605X/acfc9d.
[46] G. M. Kim, K. H. T. Le, S. M. Giannitelli, Y. J. Lee, A. Rainer, and M. Trombetta, "Electrospinning of PCL/PVP blends for tissue engineering scaffolds," *J. Mater. Sci. Mater. Med.*, vol. 24, no. 6, pp. 1425–1442, 2013, doi: 10.1007/s10856-013-4893-6.
[47] M. Çapkin *et al.*, "Random/aligned electrospun PCL/PCL-collagen nanofibrous

membranes: Comparison of neural differentiation of rat AdMSCs and BMSCs," *Biomed. Mater.*, vol. 7, no. 4, 2012, doi: 10.1088/1748-6041/7/4/045013.
[48] B. Massoumi, M. Ramezani, M. Jaymand, and M. Ahmadinejad, "Multi-walled carbon nanotubes-g-[poly(ethylene glycol)-b-poly(ε-caprolactone)]: synthesis, characterization, and properties," *J. Polym. Res.*, vol. 22, no. 11, 2015, doi: 10.1007/s10965-015-0863-7.
[49] M. C. Techniques, "3. Infrared spectroscopy."
[50] A. Marmur, C. Della Volpe, S. Siboni, A. Amirfazli, and J. W. Drelich, "Contact angles and wettability: Towards common and accurate terminology," *Surf. Innov.*, vol. 5, no. 1, pp. 3–8, 2017, doi: 10.1680/jsuin.17.00002.
[51] J. W. Biggers *et al.*, "Autophagy, cell death and sustained senescence arrest in B16/F10 melanoma cells and HCT-116 colon carcinoma cells in response to the novel microtubule poison, JG-03-14," *Cancer Chemother. Pharmacol.*, vol. 71, no. 2, pp. 441–455, 2013, doi: 10.1007/s00280-012-2024-6.
[52] J. S. Khalili *et al.*, "Combination small molecule MEK and PI3K inhibition enhances uveal melanoma cell death in a mutant GNAQ- and GNA11-dependent manner," *Clin. Cancer Res.*, vol. 18, no. 16, pp. 4345–4355, 2012, doi: 10.1158/1078-0432.CCR-11-3227.
[53] C. Krepler *et al.*, "A Comprehensive Patient-Derived Xenograft Collection Representing the Heterogeneity of Melanoma," *Cell Rep.*, vol. 21, no. 7, pp. 1953–1967, 2017, doi: 10.1016/j.celrep.2017.10.021.
[54] S. Guo *et al.*, "Sestrin2 contributes to BRAF inhibitor resistance via reducing redox vulnerability of melanoma cells," *J. Dermatol. Sci.*, vol. 109, no. 2, pp. 52–60, 2023, doi: 10.1016/j.jdermsci.2022.12.007.
[55] Y. S. Choi *et al.*, "Topical therapy for regression and melanoma prevention of congenital giant nevi," *Cell*, vol. 185, no. 12, pp. 2071-2085.e12, 2022, doi: 10.1016/j.cell.2022.04.025.
[56] S. H. Abbas, A. A. Abd El-Hafeez, M. E. Shoman, M. M. Montano, and H. A. Hassan, "New quinoline/chalcone hybrids as anti-cancer agents: Design, synthesis, and evaluations of cytotoxicity and PI3K inhibitory activity," *Bioorg. Chem.*, vol. 82, no. November 2018, pp. 360–377, 2019, doi: 10.1016/j.bioorg.2018.10.064.